

Synaptic Circuits Involving an Individual Retinogeniculate Axon in the Cat

JAMES E. HAMOS, SUSAN C. VAN HORN, DENIS RACZKOWSKI,
AND S. MURRAY SHERMAN

Department of Neurobiology and Behavior, State University of New York at
Stony Brook, Stony Brook, New York 11794-5230

ABSTRACT

In order to describe the circuitry of a single retinal X-cell axon in the lateral geniculate nucleus, we physiologically characterized such an axon in the optic tract and injected it intra-axonally with horseradish peroxidase. Subsequently, we recovered the axon and employed electron microscopic techniques to examine the distribution of synapses from 18% of its labeled terminals by reconstructing the unlabeled postsynaptic neurons through a series of 1,200 consecutive thin sections. We found remarkable selectivity for the axon's output, since only four of the 43 available neurons in a limited portion of the terminal arbor receive synapses from labeled terminals. Moreover, the distribution of these synapses on the four neurons, which we term *cells 1* through *4*, varies with respect to synapses from other classes of terminals that contact the same cells, including synapses from unlabeled retinal terminals. For *cells 1* and *3*, the labeled terminals provide 49% and 33%, respectively, of their retinal synapses, and these are located on both dendritic shafts and appendages. Synapses from the injected axon to these cells are thus integrated with those from other retinal axons. For *cell 2*, the labeled terminals provide 100% of its retinal synapses, but these synapses converge on clusters of dendritic appendages where they are integrated with convergent inhibitory inputs. Finally, for *cell 4*, the labeled terminals provide less than 2% of its retinal inputs, and these are distally located; we suggest that these synapses are remnants of physiologically inappropriate miswiring that occurs during development. The findings from this study support a concept of selectivity in neuronal circuitry in the mammalian central nervous system and also reveal some of the diverse integrative properties of neurons in the lateral geniculate nucleus.

Key words: lateral geniculate nucleus, synaptic connections, visual pathways, electron microscopy

Laminae A and A1 of the cat's lateral geniculate nucleus represent a useful model system for studying the neuroanatomical basis of sensory neural processing (Guillery, '69a,b; Famiglietti and Peters, '72; LeVay and Ferster, '77; Singer, '77; Friedlander et al., '81; Fitzpatrick et al., '84; Wilson et al., '84). Much attention has been focused on the parallel X- and Y-cell pathways that originate in the retina and are processed through laminae A and A1 prior to their separate projection to visual cortex (Stone et al., '79; Sherman and Spear, '82; Sherman, '85a). Furthermore, the synaptic morphology of the lateral geniculate nucleus comprises a relatively small number of readily identifiable classes of synaptic terminal (Guillery, '69a,b; Famiglietti and Peters, '72). These include the retinal terminals, which have been unambiguously characterized and are particularly easy to

identify (Peters and Palay, '66; Guillery, '69a,b; Famiglietti and Peters, '72; Szentágothai, '73; Robson and Mason, '79). Finally, recent studies have examined some of the differences in the synaptology of geniculate X- and Y-cells (Mason et al., '84; Wilson et al., '84; Hamos et al., '85; Van Horn et al., '85).

While a great deal has been learned about geniculate circuitry with respect to connections made by populations of synaptic terminals (e.g., from retina, from cortex, and

Accepted September 18, 1986.

Address reprint requests to James E. Hamos, Department of Neurology, University of Massachusetts Medical Center, 55 Lake Avenue North, Worcester, MA 01605.

from intrinsic sources), little is known about the patterns of synapses from individual axons to the dendritic arbors of geniculate neurons. Such information is especially significant for the synapses from retinogeniculate axons, because these afferent axons effectively activate geniculate neurons. Each of these axons has an extensive terminal arborization with hundreds of presynaptic terminals of varying size and shape (Bowling and Michael, '80, '84; Sur and Sherman, '82). Knowledge of the spatial distribution of synapses from single retinal axons onto geniculate neurons is a prerequisite to the complete understanding of retinogeniculate transmission and the relay of retinal information to the visual cortex. Such knowledge would also help to explain some of the response properties of geniculate cells that depend on circuitry within the lateral geniculate nucleus itself.

As a first effort to characterize patterns of connections from individual afferent axons to geniculate neurons, we studied some of the synaptic circuits of a single retinal X-cell axon. This was achieved by recording intracellularly from that axon, iontophoresing horseradish peroxidase (HRP) into it, and subsequently adopting electron microscopic reconstruction techniques to determine the distribution of the synapses formed by HRP-labeled terminals onto their postsynaptic cells. We have found remarkable selectivity in the number of neurons contacted by the single, labeled axon as well as diversity in the patterns of synaptic connections onto each of these neurons. The axon establishes multiple synaptic contacts with the processes of a few cells within its terminal field while bypassing all of the dendrites from many neighboring neurons. Also, each of the identified postsynaptic targets is morphologically quite distinct from the others, a distinction that includes the pattern of synaptic inputs from both labeled and unlabeled terminals. These data provide insights into the organization of retinogeniculate circuitry involving the X-cell pathway.

MATERIALS AND METHODS

General physiological and morphological methods

The methods used for recording from an optic tract axon, filling it with HRP, and subsequently recovering the axon for anatomical examination have been fully documented in previous publications from this laboratory (Friedlander et al., '81; Sur et al., '82; Sur and Sherman, '82; Sur et al., '84; Humphrey et al., '85a,b). A brief outline of these methods follows.

A normal, adult cat was anesthetized, paralyzed, and artificially respired. For anesthesia, we employed halothane during the initial surgical procedures and a combination of N₂O/O₂ and barbiturates during the physiological examination that followed. The cat's core temperature, expired CO₂, and heart rate were monitored throughout to ensure the quality of the preparation and the depth of anesthesia. The pupils were dilated and nictitating membranes were retracted with topical application of drugs, and contact lenses were fitted to focus the retina on the visual stimuli presented during recording. We placed a hydraulically sealed chamber over a craniotomy through which our recording electrodes could be advanced. Stimulating electrodes were inserted across the optic chiasm to orthodromically activate optic tract axons. We recorded the activity of such axons ventral to the lateral geniculate nucleus with fine micropipettes that were previously filled with 3% HRP and 0.3 M KCl and then beveled to a final impedance of

120 MΩ at 100 Hz. This corresponds to a tip diameter of roughly 0.2–0.5 μm.

Visual stimuli consisted of various bright and dark targets moved or flashed onto a frontal tangent screen plus drifting or sinusoidally counterphased sinewave gratings generated on a cathode ray tube under computer control. The gratings had a mean luminance of 40 cd/m², and their spatial and temporal frequencies could be continuously varied. We could also continuously vary both the contrast from 0 to 0.6 as well as the spatial phase of a counterphased grating. Responses to the grating could be averaged and Fourier-analyzed with the aid of our computer. Such analysis of responses to counterphased gratings produces a measure of the linear and nonlinear response components of recorded axons or cells. This response property was one of several measures used to characterize each optic tract axon encountered as deriving from a retinal X- or Y-cell (Hochstein and Shapley, '76). The other measures were latency of response to optic chiasm shock, receptive field center size, tonic or phasic nature of the response to stimulation of the center, and responsiveness of the cell to large targets moved rapidly through its receptive field (Cleland et al., '71; Hoffmann et al., '72).

The axon described in the present paper was identified as a retinal X-cell axon on the basis of its responses to the above-mentioned tests (see Results). After we studied the extracellular response properties of the axon, we penetrated it, confirmed that it was the same axon that we recorded extracellularly by matching key properties, and iontophoresed HRP into the axon with brief depolarizing pulses. These pulses were administered via a 25–50% duty cycle at 10 Hz with an amplitude of 2–10 nA for 30 seconds. Ten hours after HRP iontophoresis, the cat was deeply anesthetized with barbiturates and perfused transcardially with fixatives (1% paraformaldehyde and 2% glutaraldehyde in a 0.15 M phosphate buffer with calcium chloride) followed by a wash (5% dextrose in phosphate buffer). The brain was then removed and refrigerated overnight in a solution of 5% dextrose in phosphate buffer.

After 10 additional hours, the lateral geniculate nucleus ipsilateral to the recording site was coronally sectioned at 50 μm on a Vibratome. These sections were treated with 3,3'-diaminobenzidine plus 1% cobaltous chloride. We then wet mounted the sections with phosphate buffer on glass slides for rapid light microscopic determination of the location of the injected axon and its terminal arbor. Portions of the lateral geniculate nucleus containing the labeled axon were osmicated, dehydrated, and embedded in plastic resin between two pieces of thin plastic.

We drew the terminal arbor of the injected axon as seen in the coronal plane with the aid of a ×100, oil-immersion objective and a drawing tube attached to a light microscope. The terminal arbor was subsequently reconstructed from six consecutive 50-μm sections. In order to minimize the amount of electron microscopic reconstruction, we selected a ventral region of the terminal arbor for electron microscopic examination, because it was wholly contained within two adjacent 50-μm blocks plus minimal parts of neighboring blocks (see Results for details). The dorsal portion of the terminal arbor remains in five 50-μm blocks.

Analysis of postsynaptic neurons

We fully sectioned the ventral portion of the injected axon's terminal arbor for electron microscopy and produced

a series of over 1,200 consecutive thin sections from two complete 50- μm blocks and limited portions of two others. Each block was first mounted onto hardened plastic resin capsules and then thin sectioned on a Sorvall MT-5000 ultramicrotome. Consecutive sections were placed on Formvar-coated slotted grids (three to five sections per grid) that were maintained in serial order. Special care was taken to preserve all sections at the interface between blocks so that neurons and their processes could be reconstructed throughout the series. All sections were stained with lead citrate and uranyl acetate.

For the majority of this study we worked at a magnification of $\times 3,250$ on a JEOL 100B electron microscope and produced micrographs with a final magnification of $\times 8,500$. At this magnification, we could determine the morphological features of synaptic terminals and their contact sites as well as analyze a wide area on each micrograph. In order to compare cell sizes, we measured the cross-sectional areas of the cell bodies, as seen in the nucleolar plane, of 124 neurons, including four neurons that proved to be postsynaptic to the injected axon, 39 additional neurons found in the region of the labeled axon's terminal arbor (see Results), and 81 randomly selected neurons from the same series of thin sections. These measurements were made from micrographs taken at a magnification of $\times 2,200$ and printed at $\times 5,750$. At this magnification, the cell bodies of nearly all of the neurons fit into a single micrograph from which we traced the outlines of their somatic membranes and measured their areas with a planimeter. To identify how many neurons were in the labeled axon's terminal arbor, we took low-magnification micrographs ($\times 100$) of every tenth section in the series and printed them at $\times 250$. At this magnification, we could locate all the cell bodies in the arbor and many of their primary dendrites.

Initially, we searched for HRP-labeled terminals and photographed these terminals through every fourth or fifth section of the series. As dendritic processes of individual neurons postsynaptic to labeled terminals were identified, additional micrographs were made to trace each of these unlabeled dendrites to their parent cell bodies. Once the neurons were identified, we then photographed additional portions of their cell bodies, axons, and dendrites. Finally, in regions where synaptic detail was complex, we returned to the series and photographed the intervening sections that were previously bypassed. This approach permitted us to move through the depth of the series rapidly without sacrificing specific detail where necessary.

We specifically concentrated on finding dendritic appendages or spines that emerged from the dendrites of each neuron, because these appendages are a major postsynaptic target for retinal synapses and have typically been used as a criterion in classifying neurons in the lateral geniculate nucleus (Guillery, '66; Famiglietti and Peters, '72; LeVay and Ferster, '77; Friedlander et al., '81; Hitchcock and Hickey, '83; Stanford et al., '83). Where there was any indication of such appendages, we photographed nearly all the thin sections in the series. Because of the relatively large size of the neck portion of dendritic appendages in the cat's lateral geniculate nucleus (i.e., 0.2–0.7 μm in diameter vs. $< 0.2 \mu\text{m}$ in diameter, and often approaching 0.1 μm , for spines on cortical neurons; see White, '79; Špaček and Hartmann, '83) and their proximity to the parent dendrite (i.e., typically within 2 μm), we were able to include most of these appendages in our reconstructions (see Evaluation of the Method in the Discussion).

The detailed reconstructions of neurons postsynaptic to the injected axon, neurons that were not labeled with HRP, were made from the micrographs printed at a magnification of $\times 8,500$. From these, we traced the outlines of the postsynaptic cells and their processes onto acetate sheets. Depending on the complexity of the postsynaptic structures, we traced outlines from between 20 and 100 successive sections onto each acetate sheet by using internal fiducial points such as axons and blood vessels cut in cross section. The precise locations of synaptic contacts onto the neurons from all varieties of synaptic terminals were color-coded and indicated on each acetate sheet, as were any distinguishing relationships among them. Overlapping acetate sheets were then aligned with each other, and a final reconstruction was drawn.

For each neuron postsynaptic to the labeled axon, we completely reconstructed those portions of its dendritic arbor that passed through the injected axon's terminal arbor. This typically yielded dendritic segments that extended over 100 μm from the parent neuron's cell body. Most important for our further analysis, this amount of reconstruction includes the zone in which practically all retinal terminals form synapses onto geniculate neurons and extends into a zone that is characterized by synapses of presumed cortical origin (Miles and Rapisardi, '82; Mason et al., '84; Wilson et al., '84). For each neuron, we also reconstructed its entire body and the proximal portion of all its primary dendrites—even those that were directed away from the injected axon's terminal arbor. Lastly we reconstructed several dendrites on each neuron that extended well beyond the labeled axon's terminal arbor to include additional details of the pattern and synaptic relationships of unlabeled terminals in this region.

In summary, although we have only partially reconstructed a selected population of neurons, the reconstructions include details of nearly all of the retinal synapses to these cells. Our criteria for limiting the reconstruction of any particular portion of a neuron's dendritic arbor were (1) that the dendrites passed from a zone of retinal inputs to one dominated by cortical inputs; (2) that the dendrites extended out of the labeled axon's terminal arbor; or (3) that the dendrites became less than 0.5 μm in diameter, which indicated that they were becoming quite distal within the dendritic arborization: retinal terminals rarely form synapses on these dendritic branches (Miles and Rapisardi, '82; Mason et al., '84, Wilson et al., '84). Therefore, although every reconstruction presented below contains dendrites that could have been followed much further, we concentrated only on completely reconstructing dendrites that passed through the region of the injected axon's terminal arbor.

Quantitative analysis

We compared the numbers and locations of synapses from the labeled retinal terminals onto the reconstructed neurons with those from other, unlabeled terminals (including unlabeled retinal terminals) that contact the same neurons. For each contact, we identified its postsynaptic target on a dendritic shaft or appendage of one of the reconstructed neurons. We then measured the distance along the intervening dendrites from that synapse to the base of the primary dendrite at the cell body; thus, we define the anatomical distance of a synapse from the soma as the distance along the dendritic path to the soma. For each neuron, we subsequently calculated the percentage of retinal synapses

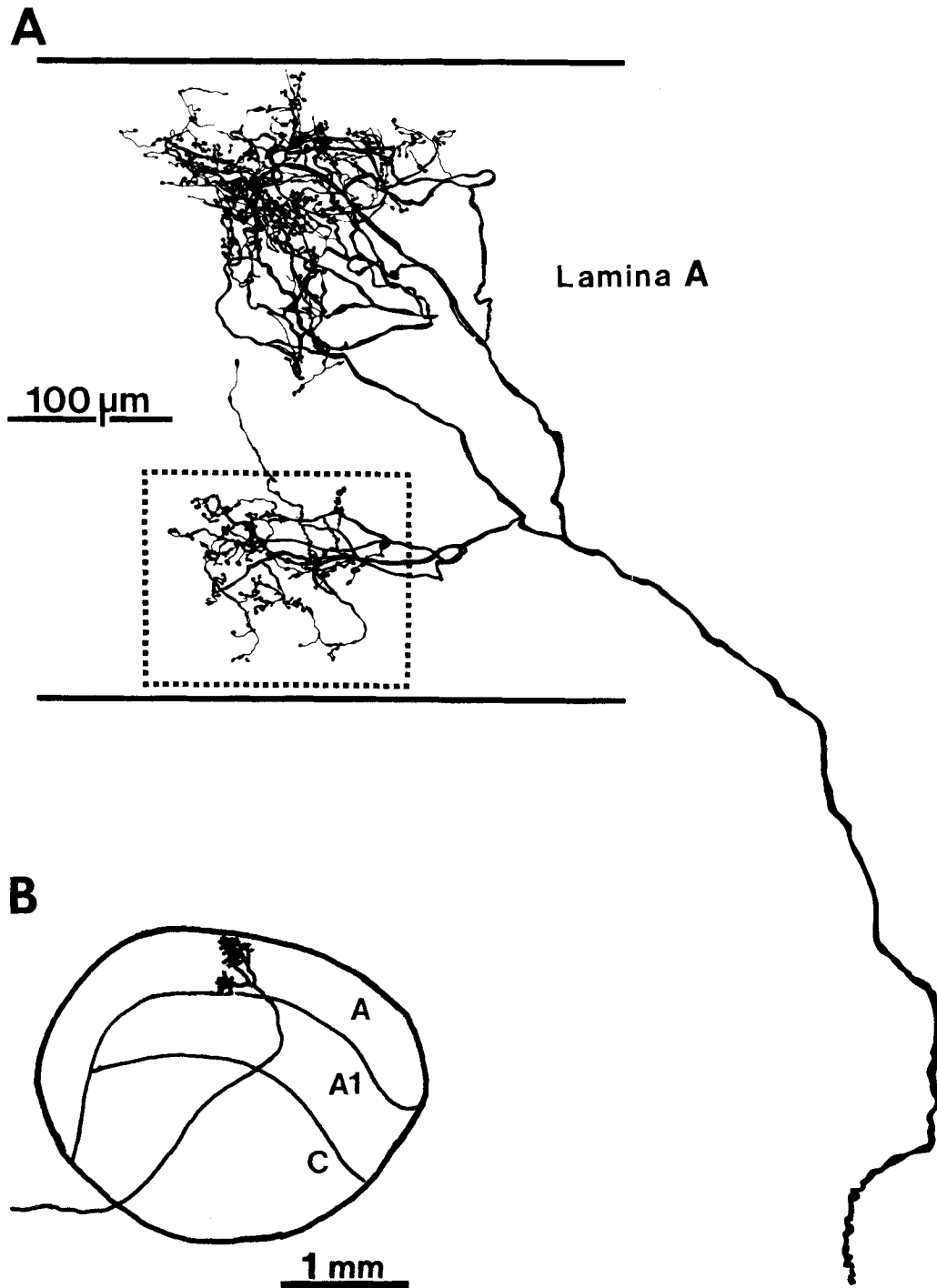


Fig. 1. Retinal X-cell arbor. A: High-power drawing from coronal sections of the terminal arborization from a retinogeniculate axon that was injected with HRP and studied with the electron microscope. Laminar boundaries are shown by solid lines. The outlined area represents a ventral region of the arborization that was completely thin-sectioned. B: Low-power drawing indicating the axon's position within lamina A of the lateral geniculate nucleus.

provided by the single, labeled axon relative to the total (labeled plus unlabeled) retinal input as well as the distribution of these contacts along the length of the neuron's dendritic arbor. This distribution was compared to that of synapses from nonretinal terminals.

Finally, we used an algorithm to convert the actual anatomical distance between each synaptic location and the soma to a relative electrotonic distance. The algorithm involved solving simple cable equations (e.g., Jack et al., '75; Rall, '77) based on our measurements of the thickness and length of various dendritic segments. This algorithm assumes a passive membrane, negligible external resistance, and constant internal and specific membrane resistances. We divided the reconstructed dendritic arbors into nontapering segments with lengths ranging from 0.8 μm to 21.7 μm . The beginning and end of each segment was either a branch point, or a point at which a curving dendrite changed directions, or the base of a dendritic appendage. These appendages were also treated like short dendritic branches ranging from 0.4 μm to 4.1 μm in length. To determine the relative electronic length of each segment, we divided its length by the square root of its diameter (Rall, '77). The relative electronic distance of each synapse from the soma is then simply the sum of all of the segmental electrotonic distances on the path from the synapse to the soma.

Statistics

Unless otherwise indicated, we employed the Mann-Whitney *U*-test for all statistical comparisons.

RESULTS

Physiology and light microscopy of the labeled axon

The labeled retinogeniculate axon was activated by visual stimulation presented to the eye contralateral to the recording site. We identified it physiologically as an X-cell axon on the basis of the battery of tests described in Materials and Methods. In particular, the axon exhibited linear spatial and temporal summation in response to gratings sinusoidally modulated in time and space, and it responded to electrical activation of the optic chiasm at a latency of 0.9 msec. The axon's receptive field had an OFF center that was 1.0° in diameter, located 10° from the vertical meridian and 16° below the horizontal zero parallel.

Figure 1 shows a reconstruction of the labeled axon's terminal arbor made at the light microscopic level. As expected from the axon's receptive field coordinates and ocular dominance (Sanderson, '71a), its terminal arbor is completely confined to lamina A in the rostral one-third of the lateral geniculate nucleus. The narrow arbor represents typical morphology for an X-cell axon (Sur and Sherman, '82; Bowling and Michael, '84). It extends 180 μm in the mediolateral direction and 370 μm in the dorsoventral axis. The maximum rostrocaudal extent of any single portion of the arborization is roughly 200 μm . With the light microscope, we counted 658 varicosities and boutons along the axon or on terminal stalks, and this is within the range of bouton numbers previously described for normal X-cell retinogeniculate arbors (Sur and Sherman, '82; Bowling and Michael, '84). We tentatively identified these boutons as synaptic terminals, and this identification was subsequently confirmed in our electron microscopic analysis (see below).

An advantageous feature of this axon is that its terminal arbor is divided into two portions such that, except for a few scattered terminals, a ventral subfield remains separated from a dorsal portion by roughly 150 μm . This sort of dorsoventral asymmetry for X-cell arbors has been described by Bowling and Michael ('84), and we have also seen other examples of such morphology for X-cell arbors (unpublished observations). Because retinal synapses typically contact dendrites of geniculate neurons within 100 μm of the soma (Miles and Rapisardi, '82; Mason et al., '84; Wilson et al., '84), it is very unlikely that a single geniculate cell can receive substantial numbers of retinal inputs from both portions of the labeled axon's arbor. Therefore, the circuitry that we analyzed in one of these separated portions of the arborization is unlikely to include neurons whose retinal recipient zones would extend into the other portion. The ventral portion of the injected axon's arbor, which we thin sectioned and subsequently examined in the electron microscope, extends 130 μm along the mediolateral axis, 110 μm along the dorsoventral axis, and roughly 100 μm along the rostrocaudal axis. All of our reconstructions were made from this ventral region that contains 117 (or 18%) of the 658 terminals identified at the light microscopic level for the entire terminal arbor.

General ultrastructural features of the neuropil

Identification of synaptic terminals. One of our aims was to compare and contrast the morphological features of the labeled retinal terminals with those of other, unlabeled terminals. To do this, we adopted the criteria described by Guillery ('69a) to characterize synaptic terminals within the cat's lateral geniculate nucleus into three major classes (Fig. 2). We identified terminal types with the aid of $\times 7$ and $\times 10$ magnifying lenses placed over our original $\times 8,500$ electron micrographs and confirmed all decisions through the many micrographs of each terminal available in the series.

Within the neuropil of the labeled axon's terminal arbor, we found examples of each of Guillery's ('69a) three broad classes of synaptic terminal (see also Peters and Palay, '66; Famiglietti and Peters, '72; Szentágothai, '73). These three terminal classes are as follows. (1) RLP terminals are so named for their round vesicles, large profiles, and pale mitochondria (Fig. 2A). They have been unambiguously identified as retinal terminals (Guillery, '69a; Szentágothai, '73; Robson and Mason, '79), and they form asymmetrical synaptic contacts. (2) RSD terminals (round vesicles, small profiles, and dark mitochondria) also form asymmetrical synapses (Fig. 2B). Many or all are thought to derive from corticogeniculate axons (Guillery, '67; Szentágothai, '73; Robson, '83; but see Wilson et al., '84). (3) F terminals (flattened or pleomorphic vesicles) form symmetrical synapses (Fig. 2). In the cat, they are thought to derive from geniculate interneurons and cells of the nearby perigeniculate nucleus (Famiglietti and Peters, '72; Sterling and Davis, '80; Fitzpatrick et al., '84; Montero and Singer, '84; Cucchiari et al., '85; Hamos et al., '85). Although many F terminals may be further subdivided according to their ultrastructural characteristics into F1 and F2 types (Guillery, '69a; Famiglietti and Peters, '72), we have treated all terminals that contain flattened or pleomorphic vesicles and that form symmetrical synapses as a single type, because the distinction between F1 and F2 terminals is not

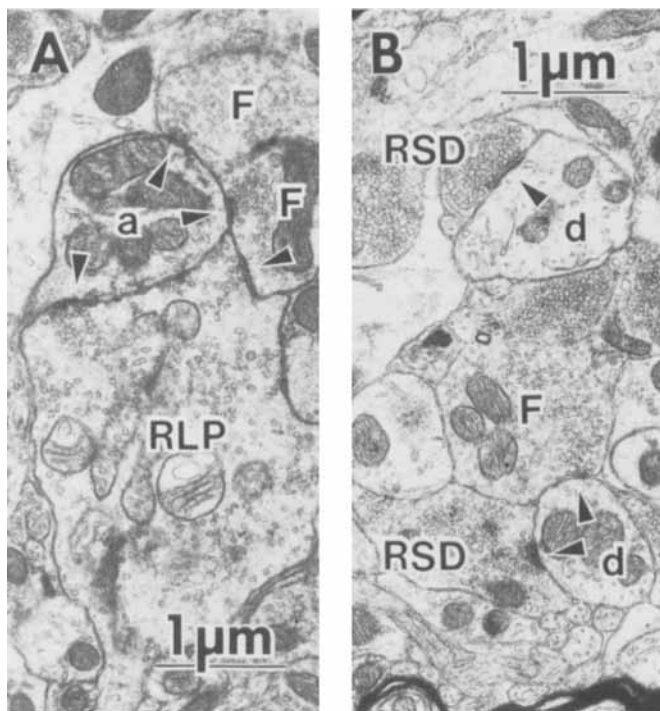


Fig. 2. Electron micrographs of representative terminals in the cat's lateral geniculate nucleus identified, as described in text, according to Guillery's ('69a) classification. In this and subsequent micrographs, synaptic sites are indicated by arrowheads directed toward the postsynaptic side of the synapse. A: RLP (round vesicles, large profiles, pale mitochondria) and F (flattened vesicles) terminals. Note that in this single section an F terminal and an RLP terminal participate in a triadic arrangement upon a dendritic appendage (a). The same appendage also receives a synapse from another F terminal. B: RSD (round vesicles, small profiles, dark mitochondrial) and F terminals. An RSD terminal located at the bottom of this figure produces an obscured synaptic site on a dendrite (d) due to an oblique plane of section; we count such contacts as synapses on the basis of the clustering of vesicles and the density of the membranes at the presumed synaptic site. The RSD terminal located at the top of this figure and the F terminal form typical asymmetrical and symmetrical synapses, respectively.

always evident. In addition to RLP, RSD, and F classes is the RLD terminal (round vesicle, large profile, and dark mitochondria; not illustrated in Fig. 2), which has been described by Famiglietti and Peters ('72) and by Ide ('82). Although RLD terminals were occasionally seen in our material, none contact any of the processes postsynaptic to the labeled axon (see below), and they are not considered further in this paper.

A feature of many RLP and F terminals in laminae A and A1 is their participation in the triadic arrangement of synapses (Peters and Palay, '66; Guillery, '69a; Famiglietti and Peters, '72; Szentágothai, '73; Rapisardi and Miles, '84; Wilson et al., '84; Hamos et al., '85), in which a retinal terminal contacts an F terminal, and both terminals contact the same postsynaptic dendrite or dendritic appendage (Fig. 2A). In a few cases, we noted single retinal terminals that are involved in more complicated synaptic triads in which the RLP terminal makes two or three contacts onto different F terminals, and all of the F terminals contact the

same postsynaptic structure. Finally, we examined whether each retinal terminal participates in a "glomerulus" (Peters and Palay, '66; Famiglietti and Peters, '72; Szentágothai, '73) or "encapsulated synaptic zone" (Guillery, '69a,b), since these structures have been a primary focus for previous studies of retinogeniculate circuitry. We found considerable variation in the complexity of glomeruli, as also described by others (Peters and Palay, '66; Guillery, '69a; Famiglietti and Peters, '72; Robson and Mason, '79). Consequently, this term may actually refer to a spectrum of structures from a fairly simple synaptic arrangements that are limited to a single triad to quite complex glomeruli that contain numerous synapses from many sources.

In addition to our classification of synaptic terminals, we sought to produce a quantitative description of the complete distribution of synapses from different varieties of terminals to specific cells in the neuropil. Therefore, when presumed synaptic contacts were sectioned in an oblique plane such that the synaptic contact zone is obscured, we included it as a synapse if its appearance was otherwise typical of a synaptic site. These are terminals in which clusters of synaptic vesicles lie opposite to an obliquely sectioned and, therefore, dense portion of membrane (Fig. 2B). We also identified the total number of synaptic contacts that each retinal terminal makes with *different* postsynaptic structures, even if these structures derive from the same cell. For this analysis, we used the approach of Somogyi et al. ('83). That is, we counted as a separate synapse each contact made between a terminal and an individual dendrite or its dendritic appendages, irrespective of the number of individual synaptic active zones made on the same postsynaptic element (see also Rapisardi and Miles, '84). By this criterion, each labeled terminal in our sample provides between one and 28 contacts to postsynaptic structures, including as many as 11 synapses to a single reconstructed postsynaptic neuron.

Appearance of labeled terminals. Electron microscopic analysis reveals that the labeled terminals from the injected axon possess morphology and synaptic connections that are typical for retinal terminals (Fig. 3), since all of the labeled synaptic profiles are conventional RLP terminals and every swelling along the labeled axon is presynaptic. No labeled structure in our material was ever seen to be postsynaptic. Although vesicles in the labeled terminals are more variable in shape than is the case for those in unlabeled RLP terminals, which is presumably an artifact of the HRP labeling (see legend to Fig. 3), other features of the labeled terminals are quite consistent with those of unlabeled RLP terminals. The mitochondria in the labeled terminals are noticeably paler than are those of neighboring structures, and this distinguishes retinal terminals (Guillery, '69a). The labeled terminals display the full range of sizes typical of retinal terminals, and these are characteristically larger than neighboring nonretinal terminals (see Retinal Terminal Morphometry below). Finally, the labeled terminals give rise to asymmetrical synaptic contacts and are presynaptic to dendritic structures (i.e., dendritic shafts and appendages) or, as members of synaptic triads, are also presynaptic to F terminals.

We identified and photographed 155 HRP-labeled terminals in our series. The increase in the number of terminals counted from the light microscope to the electron microscope (i.e., 117 vs. 155) can be accounted for by the small size of some of the labeled axon's varicosities. Many of the

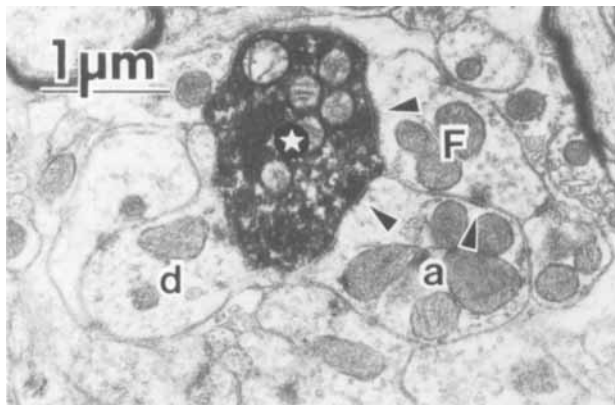


Fig. 3. Electron micrograph of a labeled terminal (star) from the injected retinogeniculate axon synapsing on a dendritic appendage (a) connected to a dendrite (d) from cell 2 (see text). This terminal, and others from the injected axon, are identified as RLP terminals because of (1) their pale mitochondria, (2) the asymmetrical synapses that they form on dendritic processes, and (3) their participation in synaptic triads with adjacent F terminals. Note the three synapses that form a triad in this single section. The variability in shape of the synaptic vesicles seen in this labeled terminal is a common feature of terminals identified after an intracellular injection of HRP into their parent axon; therefore, the shape of vesicles in labeled terminals is not a meaningful morphological feature for this type of tissue.

labeled terminals (41 of 155) are less than $2.0 \mu\text{m}$ in maximum diameter and exhibit myelinated pre- and post-terminal segments. This indicates that the terminals are boutons *en passant* along axons that themselves are roughly $1.0 \mu\text{m}$ in diameter. The difference in sizes between each of these small labeled terminals and its parent axon would have been extremely difficult to detect with the resolving power of the light microscope. Our discovery of more terminals with the electron microscope than with the light microscope also suggests that we have omitted few, if any, labeled terminals in our electron microscopic reconstructions.

Features of neurons innervated by the labeled axon

Identification of postsynaptic cells. Because the vast bulk of retinal terminals are located on dendrites of geniculate cells within $100 \mu\text{m}$ of the soma (Miles and Rapisardi, '82; Mason et al., '84; Wilson et al., '84), we found it possible to reconstruct to parent cell bodies most processes that are postsynaptic to labeled terminals. Extensive analysis of the neurons postsynaptic to the labeled axon suggests considerable complexity in retinogeniculate circuitry. We reconstructed four neurons whose dendrites are the postsynaptic targets for 113 (or 73%) of the 155 labeled terminals. Figure 4 shows a reconstruction of the location of the cell bodies of each of the four postsynaptic cells relative to the labeled terminal arbor as well as to nearby geniculate neurons that received no detectable input from the labeled axon.

The 113 labeled terminals that contact the above-mentioned four neurons provide 343 total synapses to dendritic shafts and appendages. We traced the postsynaptic targets of 260 (or 76%) of these synapses to larger dendrites and ultimately to the four parent cell bodies. The remaining synapses are primarily located on appendages whose fine neck portions were lost in the reconstruction. In addition,

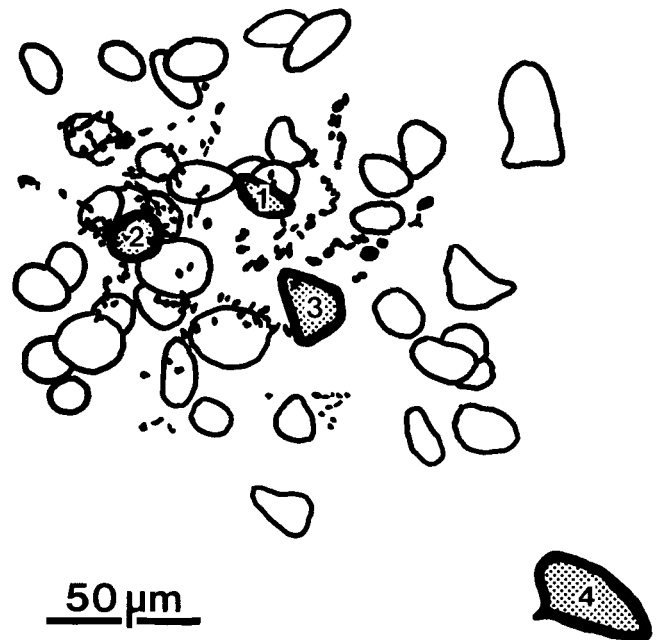


Fig. 4. Two-dimensional drawing of the 117 labeled terminals from the injected axon's ventral region (outlined in Fig. 1) superimposed over the positions of all the neurons whose somata or dendrites impinge on the terminal field. The positions of these 43 neurons were determined from low-magnification electron micrographs. The four neurons indicated receive multiple innervation from labeled terminals and were extensively reconstructed from higher-magnification electron micrographs to determine their innervation patterns from labeled and unlabeled terminals. Numbers shown for the reconstructed neurons represent the means of identification for the neurons throughout the text.

the 42 labeled terminals that do not contact reconstructed portions of the four neurons provide multiple innervation to individual dendritic shafts or appendages that we traced only to a limited degree, since the dendrites left the labeled axon's terminal arbor. These other dendrites may either belong to portions of the four reconstructed neurons, connecting with them in regions not reconstructed, or they may belong to one or more other neurons that we were unable to reconstruct to their cell bodies (see Discussion).

With regard to the synaptic contacts made by individual retinal terminals, we distinguished between those formed onto dendritic shafts and appendages and those formed onto F terminals. Most or all of these postsynaptic F terminals are terminals that originate from the dendrites of local circuit neurons or interneurons (Famiglietti and Peters, '72; Hamos et al., '85). However, due to the length and extremely fine caliber of the processes that connect these F terminals with one another and with their parent dendrites, it is not feasible to reconstruct the unlabeled F terminals to their parent dendrites (Rapisardi and Miles, '84; Hamos et al., '85). We thus cannot provide quantitative estimates of the pattern of contacts by the labeled axon to interneurons via these F terminals, although we can describe the pattern of synapses from the F terminals to other reconstructed processes. Consequently, we focus below on the morphological basis of transmission of retinal input to presumptive geniculate projection cells that are the source

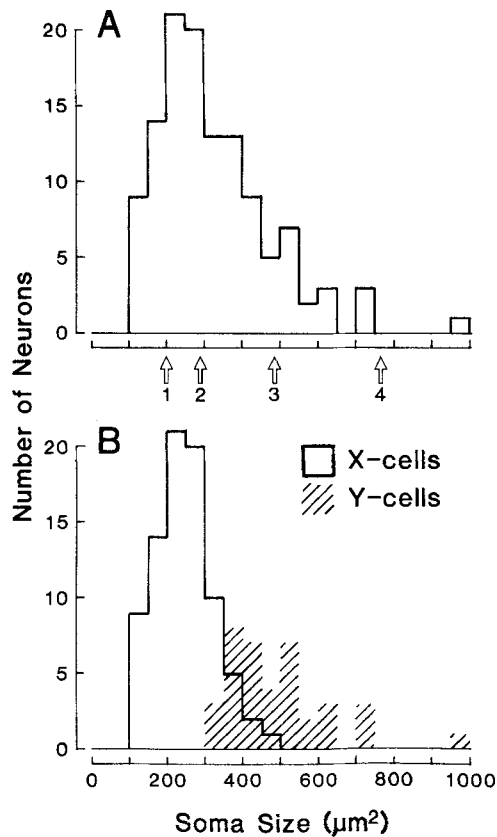


Fig. 5.A: Soma size histogram of 124 neurons including the 43 neurons whose somata and/or dendrites impinge on the ventral region of the injected axon (see Fig. 4) and an additional 81 randomly selected neurons that were found in the same resin-embedded blocks of the lateral geniculate nucleus. Sizes and identifying numbers of the four neurons postsynaptic to labeled terminals are indicated by open arrows. B: Same data as in A recomputed by using the data of Friedlander et al. ('81) to suggest subpopulations of our measured neurons as X- or Y-cells. To make this comparison, we recalculated the data of Friedlander et al. ('81) by including a correction of 15% between the mean cross-sectional areas of their 1,246 soma sizes, measured with the light microscope from Nissl-stained sections, and the mean areas of our 124 neurons, measured from thin sections prepared for electron microscopy. Since they physiologically identified their neurons, we then determined a relative percentage of X- and Y-cells in each 50 μm bin. This comparison indicates that the soma sizes of cells 1 and 2 lie exclusively in the X-cell range, that of cell 3 lies in the overlap region between X- and Y-cells, and that of cell 4 lies exclusively in the Y-cell range.

of the postsynaptic dendritic shafts and appendages and that we are able to reconstruct to their cell bodies. Unless otherwise indicated, the following quantitative descriptions of the postsynaptic relationships formed by the labeled axon include the postsynaptic F terminals only in relation to their participation in synaptic triads.

Classification of postsynaptic neurons. Recent structure/function studies have identified certain morphological features and synaptic relationships of geniculate neurons identified as X- or Y-cells that project an axon to cortex (Friedlander et al., '81; Wilson et al., '84; Van Horn et al., '85). X-cells have smaller cell bodies and thinner, more curved dendrites than do Y-cells. Compared to Y-cells, X-cells tend to have more dendritic appendages, more retinal inputs to these appendages than to the neighboring den-

TABLE 1. Features of Neurons Postsynaptic to Retinal X-Cell Axon

Feature	Cell 1	Cell 2	Cell 3	Cell 4
Maximum area of soma (μm^2)	200	290	485	765
No. of 1° dendrites				
Total	5	3	7	7
Innervated by labeled axon directly or via daughter branch	2	3	4	2
Synaptic inputs identified on reconstructed neurons				
Total	224	856	952	1,842
From labeled RLP	21	176	51	12
On appendages	15	146	20	6
In triads	15	160	45	2
From unlabeled RLP	22	0	104	182
On appendages	12	0	34	44
In triads	18	0	51	16
From F	165	541	422	514
On appendages	53	313	82	44
On soma	7	10	40	55
From RSD	16	139	375	1,134
On appendages	0	40	2	1
On soma	1	1	11	25

driftic shafts, and more frequent retinal inputs involved in synaptic triads. We used this set of observations to characterize as an X- or Y-cell each of the four geniculate cells postsynaptic to the labeled retinal axon (see below). Finally, because LeVay and Ferster ('77) have suggested that the cell bodies of X-cells projecting to cortex contain cytoplasmic laminated bodies, we have searched for this feature in each of the reconstructed neurons. We found such a cytoplasmic laminated body in the soma of only one of the four neurons postsynaptic to the labeled axon.

Soma size is a particularly useful index of geniculate cell class (Friedlander et al., '81). From our material, we measured the cross-sectional areas of the cell bodies, as seen in the nucleolar plane, of 124 neurons (see Materials and Methods), including the four neurons that proved to be postsynaptic to the labeled axon and other neurons available in our series. To determine reasonable soma size ranges for geniculate X- and Y-cells in our distribution, we compared our measurements with those of Friedlander et al. ('81). Figure 5 shows the soma size distribution, the estimated size ranges for geniculate X- and Y-cells, and the sizes of each of the four cells postsynaptic to the labeled axon.

Distribution of synapses onto postsynaptic cells

The synapses from labeled terminals are not restricted to any single type of postsynaptic relationship with the four reconstructed neurons. Rather, they contact both dendritic shafts and appendages; they participate in synaptic triads to varying degrees; and they enter into complex synaptic arrangements, such as glomeruli, as well as simple ones. Furthermore, the neurons postsynaptic to the labeled axon vary in many morphological features, including soma size, dendritic structure, and pattern of synaptic inputs. We describe the reconstructed neurons in their ascending order of size (Table 1).

Cell 1. The small soma of cell 1, which is 200 μm^2 in cross-sectional area, falls entirely within the size distribution of geniculate X-cells (Fig. 5). It also contains a cytoplasmic laminated body. The cell has thin, curved dendrites with appendages, and the majority of retinal terminals

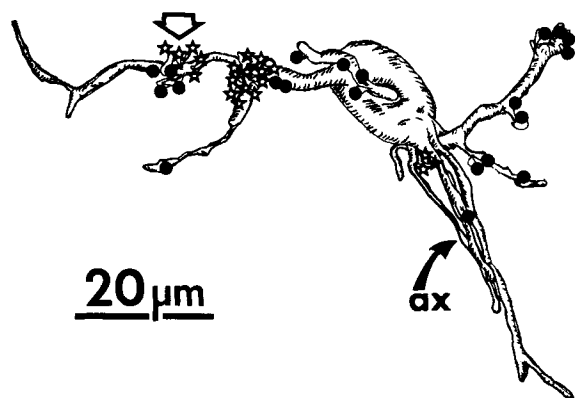


Fig. 6. Low-power reconstruction of the dendrites and axon (ax) of *cell 1* illustrating the locations of synapses from labeled terminals (open stars) and unlabeled RLP terminals (filled circles). The open arrow refers to the area detailed in Figure 7. In this and all subsequent reconstructions, every dendrite could have been traced further but we limited the reconstructions for reasons explained in the text.

contacting this neuron participate in synaptic triads, many of which are located on dendritic appendages. These features clearly indicate that *cell 1* is an X-cell.

The cell body is located near the center of the ventral portion of the labeled axon's terminal arbor (Fig. 4). Figure 6 illustrates our reconstruction of *cell 1*. Five primary dendrites arise from the oval cell body in a bipolar fashion with two directed dorsally and three ventrally. The dendritic appendages are mostly restricted to the secondary and tertiary branches of the two largest primary dendrites. Although the small cell body is in the center of the region analyzed in this study, we have limited our reconstruction of *cell 1* because its dendrites leave the terminal arbor of the injected axon and most of these dendrites at this point are less than $0.5 \mu\text{m}$ in diameter. A thin axon roughly $0.9 \mu\text{m}$ in diameter emerges from one of the ventrally directed dendrites (Fig. 6, ax), and it becomes myelinated $11 \mu\text{m}$ from the soma.

Cell 1 is sparsely innervated, including only 43 synapses from retinal terminals. Of these, the labeled axon provides 21 (or 49%) synapses. Labeled terminals contact the appendages and shafts of the secondary and tertiary branches from the two large primary dendrites that are also the prime targets for most of the unlabeled retinal input to this cell. Figure 7 shows details of the synaptic input to portions of these dendrites. The other three primary dendrites and their branches receive few contacts from any terminal type within the area reconstructed, and they receive only 12% of the retinal synapses that contact *cell 1*. Finally, 27 (or 61%) of the 43 retinal synapses onto *cell 1* are located on dendritic appendages. This includes 15 (or 71%) of the 21 synapses from labeled terminals and 12 (or 55%) of the 22 synapses from unlabeled retinal terminals (Fig. 6).

The 21 retinal synapses from labeled terminals contact dendrites within $37 \mu\text{m}$ of the soma of *cell 1* (Fig. 8) and are restricted to three clusters of synapses from nine terminals. Four of these synapses contact dendritic appendages located near the branch point of a large, ventrally directed dendrite. Twelve additional synapses are concentrated on

seven appendages and the shaft of a dendrite near the branch point of a secondary, dorsally directed dendrite. The remaining five synapses from labeled terminals contact a cluster of six dendritic appendages along another secondary dendrite that heads dorsally (Fig. 7A).

Retinal synapses innervating *cell 1* usually participate in synaptic triads. This includes 15 (or 71%) of the 21 synapses from the labeled axon and 18 (or 82%) of the 22 synapses from unlabeled retinal terminals. In addition, nine of these retinal synapses (five labeled and four unlabeled) participate in complex triads involving two or three postsynaptic F terminals. The sole presynaptic input to dendrite appendages of *cell 1* comes from the RLP and F terminals that participate in triads (Fig. 7). Consequently, retinal terminals contacting *cell 1* are involved in relatively simple glomeruli that include only the postsynaptic dendritic appendages and its presynaptic triadic inputs. Few additional synapses are present in the immediate vicinity. This contrasts with more complex synaptic glomeruli seen on another of the neurons, *cell 2*, that is postsynaptic to the labeled axon.

Synapses from both nonretinal as well as retinal sources are sparse on *cell 1*, especially when compared to the density of synapses found on equivalent regions of other geniculate neurons (see below). All of the synapses from retinal terminals are located between $13 \mu\text{m}$ and $44 \mu\text{m}$ from the soma. As is typical for geniculate cells (Guillery, '69a,b; Miles and Rapisardi, '82; Wilson et al., '84), the synapses from F terminals are concentrated close to the cell body and predominate on the soma. RSD terminals provide only a minor input to this neuron. There is, therefore, no apparent shift on the dendrites from a proximal zone of retinal synapses to a more distal one of synapses from RSD terminals, as is true for many geniculate cells (see below; Wilson et al., '84). Figure 8 summarizes the distribution of synapses from the three terminal classes onto the reconstructed portions of *cell 1*.

Cell 2. We suggest that *cell 2* is an X-cell as evidenced by the size of its soma ($290 \mu\text{m}^2$ in cross-sectional area) that falls in the X-cell range (Fig. 5), and its curved dendrites that display numerous appendages that are postsynaptic to synaptic triads. It does not contain a cytoplasmic laminated body.

The soma of *cell 2* is located rostrally in the labeled axon's terminal arbor (Fig. 4). We completely reconstructed its three primary dendrites to tertiary and quaternary branches extending roughly $100 \mu\text{m}$ from the soma (Fig. 9). The dendrites of *cell 2* have clusters of three to 12 appendages that are not located at or near major branch points. Rather, for 12 of the 18 clusters of appendages, the dendritic shaft emits small, appendage-bearing branches (Fig. 10A, br). Interestingly, beyond the final cluster of appendages, the dendritic shafts become very thin ($<0.5 \mu\text{m}$ in diameter) and leave the domain of the labeled axon's terminal arbor. This pattern indicates that we have reconstructed each of this cell's primary dendrites beyond the point of their clustered appendages and perhaps beyond all of the cell's zone of retinal input (see below). As a further check, we followed four dendrites of *cell 2* for an additional $10\text{--}50 \mu\text{m}$ beyond the points where they leave the labeled axon's terminal arbor, although the fine caliber of these peripheral dendrites makes them difficult to trace. These dendritic segments never acquire additional appendages but instead receive a sparse, nonretinal synaptic innervation. Finally,

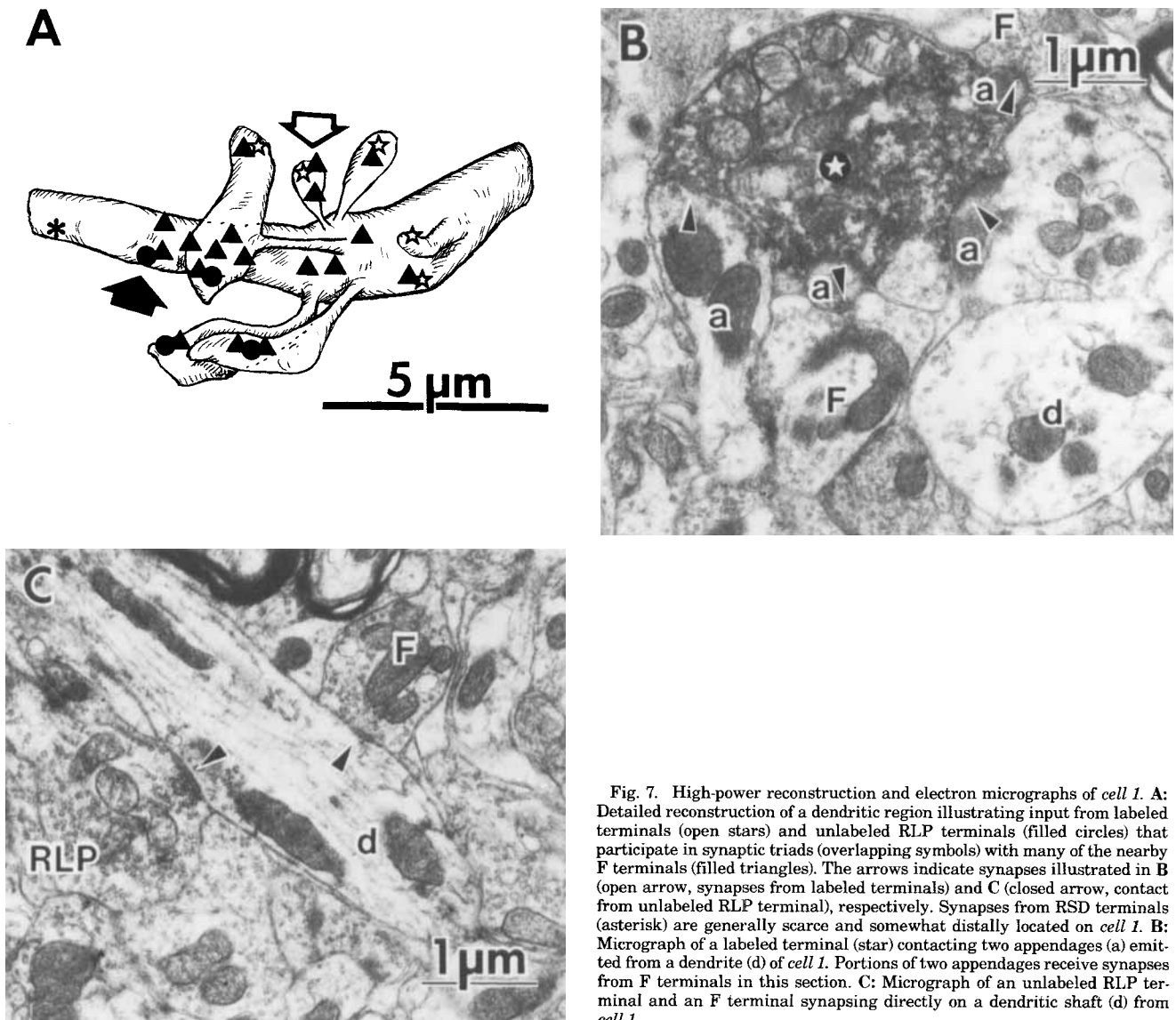


Fig. 7. High-power reconstruction and electron micrographs of *cell 1*. **A:** Detailed reconstruction of a dendritic region illustrating input from labeled terminals (open stars) and unlabeled RLP terminals (filled circles) that participate in synaptic triads (overlapping symbols) with many of the nearby F terminals (filled triangles). The arrows indicate synapses illustrated in **B** (open arrow, synapses from labeled terminals) and **C** (closed arrow, contact from unlabeled RLP terminal), respectively. Synapses from RSD terminals (asterisk) are generally scarce and somewhat distally located on *cell 1*. **B:** Micrograph of a labeled terminal (star) contacting two appendages (a) emitted from a dendrite (d) of *cell 1*. Portions of two appendages receive synapses from F terminals in this section. **C:** Micrograph of an unlabeled RLP terminal and an F terminal synapsing directly on a dendritic shaft (d) from *cell 1*.

an axon issues from the soma of *cell 2*, but it is not illustrated in Figure 9 because it is directed rostrally beyond the labeled axon's ventral terminal arbor and thus is obscured by the soma.

Every one of the 176 retinal synapses to *cell 2* is provided by the single, labeled axon. These synapses derive from 59 labeled retinal terminals. Nearly all of the retinal synapses (175 of 176) are limited to dendritic regions with clusters of appendages (Figs. 9, 10) contacting both the dendritic appendages (146 synapses) and adjacent dendritic shafts (29 synapses). A single synapse from a labeled terminal is located on an isolated tertiary dendrite of the neuron. Retinal terminals contact neither the primary dendrites of *cell 2* nor the dendritic segments between the clusters of appendages.

There is no distinct distribution of synapses from labeled terminals relative to distance from the soma of *cell 2* (Fig. 11). Rather, these contacts are restricted to regions of clustered dendritic appendages (Fig. 9) that are present at variable distances (25–85 μm from the soma) on second- through seventh-order dendrites. Each of the clusters of dendritic appendages receives input from one to eight of the labeled retinal terminals. Certain features of these terminals that innervate *cell 2* distinguish them from other terminals of the labeled axon (see Retinal Terminal Morphometry below).

Of the 176 retinal synapses innervating *cell 2*, 160 (or 91%) participate in synaptic triads. Thirty of these participate in complex triads with two or more F terminals. In addition, each dendritic appendage of *cell 2* receives not only triadic input (Fig. 3) but numerous other synapses as

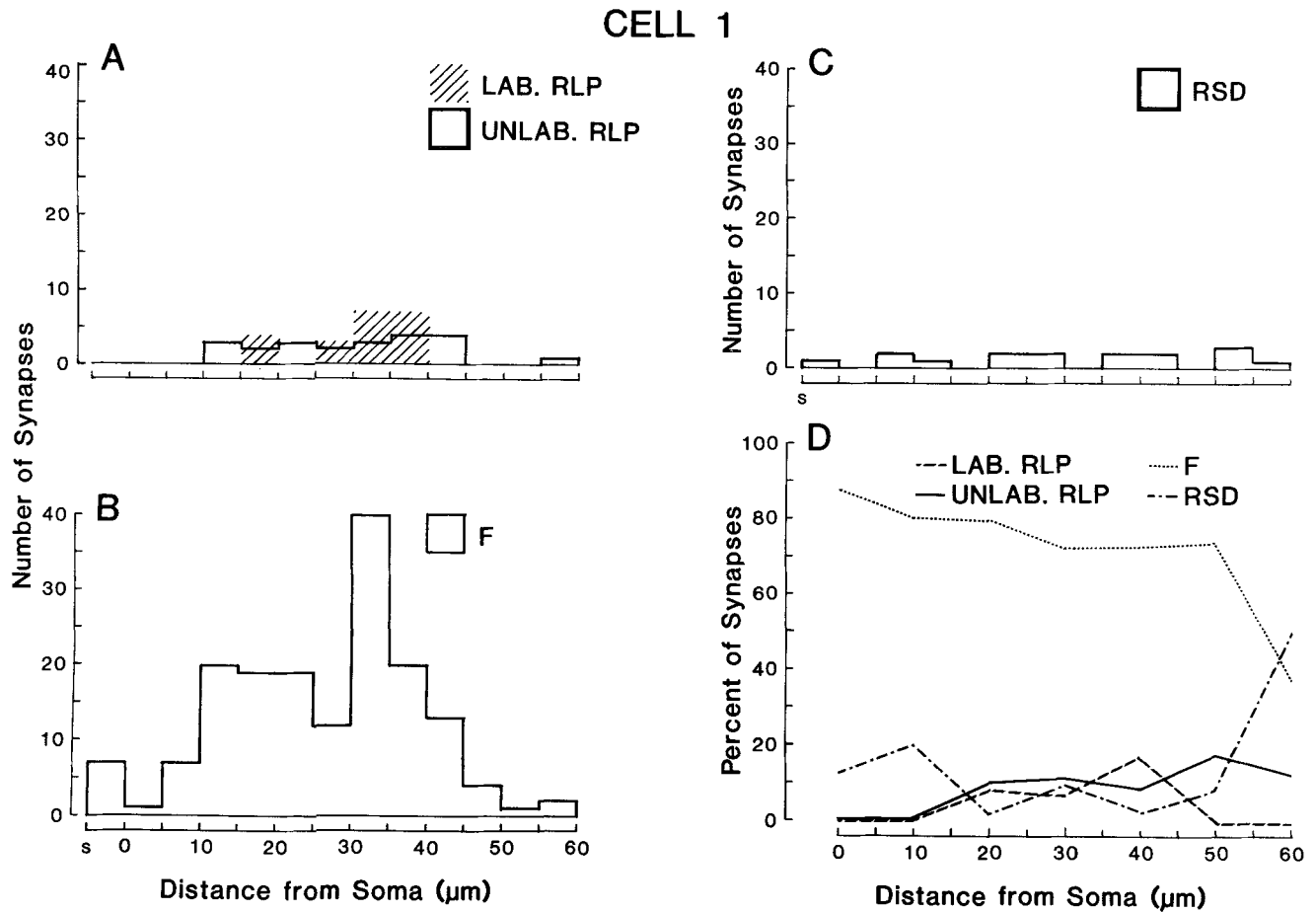


Fig. 8. Graphs showing distributions of synapses from different terminal populations along the dendrites of *cell 1*. Histograms are shown for synapses from labeled and unlabeled retinal terminals (LAB. RLP and UNLAB. RLP, respectively, in A), from F terminals (in B), and from RSD terminals (in C). Bins indicated as S represent synaptic input to the soma. The distribution plot in D illustrates the percentage of synapses from each terminal variety relative to the total number of synapses within the varying dendritic regions. Somatic inputs in D correspond to the zero distance while all other measurements are along the dendritic shaft and its appendages.

well, including those from one, two, or three nontriadic F terminals and often one or two RSD terminals (Fig. 10). For the other reconstructed cells, RSD terminals rarely contact dendritic appendages, yet for *cell 2*, 40 (or 29%) of its 139 synapses from RSD terminals are located on appendages. Because of these relationships, the innervation from RSD terminals to *cell 2* overlies that from retinal terminals (Fig. 11) whereas these distributions are separated on the other reconstructed cells.

Dendritic shafts within 5 μm of the appendages of *cell 2* are common targets for all terminal varieties, including labeled retinal terminals that participate in triads. Presumably because of the high synaptic density associated with the dendritic clusters, which are also the postsynaptic targets of synapses from the labeled axon, labeled terminals contacting *cell 2* participate in complex synaptic glomeruli. These glomeruli include synaptic triads as well as other synaptic inputs that funnel into the same region of dendritic appendages (Fig. 10).

The soma, primary dendrites, and dendritic shafts beyond 5 μm from the clustered appendages receive only 178 (or

21%) of the 856 total synapses reconstructed on *cell 2*. Of these synapses, F terminals provide ten of the 11 synapses on the soma and 38 of the 48 synapses on proximal portions of the dendrites, while 25 synapses from F terminals and five synapses from RSD terminals are on dendritic shafts between the clustered appendages. Distal to the last cluster of appendages, RSD terminals predominate, providing 57 (or 63%) of the 89 synapses. Figure 11 summarizes the distribution of synapses onto the reconstructed portions of *cell 2*.

Cell 3. *Cell 3* has a soma that is 485 μm^2 in cross-sectional area and that does not contain a cytoplasmic laminated body. Although its soma size falls in the overlap range between X- and Y-cells (Fig. 5), other data suggest that *cell 3* is an X-cell. That is, most of its retinal input participates in synaptic triads, and its curved dendrites exhibit numerous appendages.

The soma of *cell 3* is located slightly caudal to the injected axon's terminal arbor, a point not apparent from the two-dimensional reconstruction in Figure 4. Seven primary dendrites emerge from the soma, including three that we exten-

sively reconstructed to sixth-order branches (Fig. 12). The numerous dendritic appendages tend to be dispersed throughout the dendritic arbor, although they are especially prevalent near branch points (e.g., Fig. 13A). An axon arises from the soma of *cell 3*. It is $1.4\ \mu\text{m}$ in diameter and becomes myelinated $23\ \mu\text{m}$ from the axon hillock on the cell body (Fig. 12, *ax*).

The labeled axon provides 51 (or 33%) of the 155 retinal synapses to *cell 3*. All except three of the retinal terminals, one labeled and two unlabeled, avoid the primary dendrites and synapse instead on shafts (98 synapses) and appendages (54 synapses) of second-through sixth-order dendritic branches (Figs. 12, 13). The majority of these retinal synapses, including all of those from labeled terminals, converge onto the arbors from four of the seven primary dendrites. Two other dendrites receive retinal synapses only from unlabeled terminals, and still another dendrite, which emerges caudally and away from the terminal arbor, receives no retinal inputs in the limited portion that we reconstructed.

Synapses from retinal terminals are distributed 10–112 μm from the soma of *cell 3* (Fig. 14). From the labeled axon, 38 retinal terminals provide the 51 synapses onto this cell. Interestingly, these synapses from labeled terminals seem to be located within a zone of retinal inputs 40–80 μm from the soma (Fig. 14). Thus, labeled terminals form 23 (or 26%) of the 88 retinal synapses within 40 μm of the cell body, 26 (or 44%) of 59 in the region 40–80 μm from the cell body, and two (or 25%) of eight beyond 80 μm from the cell body. This trend is statistically significant ($P < .01$ on a chi-square test) and implies that labeled terminals do not form synapses randomly within the entire region of retinal inputs.

Many retinal inputs to *cell 3* participate in synaptic triads (Fig. 13). However, significantly more of the synapses from labeled terminals are parts of triads than is the case for those from unlabeled retinal terminals. This amounts to 45 (or 88%) of the 51 synapses from labeled terminals versus 51 (or 49%) of the 104 synapses from unlabeled RLP terminals ($P < .001$ on a chi-square test). When labeled or unlabeled retinal terminals synapse on dendritic appendages of *cell 3*, the two (or, rarely, three) synapses that form the triad are the sole presynaptic elements to the appendages. This is similar to the triadic innervation seen on the dendritic appendages of *cell 1*, and likewise, the retinal terminals innervating *cell 3* participate in simple synaptic glomeruli. These features are quite different from those seen on the appendages of *cell 2*, since *cell 2* receives both triadic and nontriadic input in rather complex synaptic glomeruli.

Figure 14 summarizes the distribution of synapses on the dendrites of *cell 3*. Beyond 112 μm from the soma, the

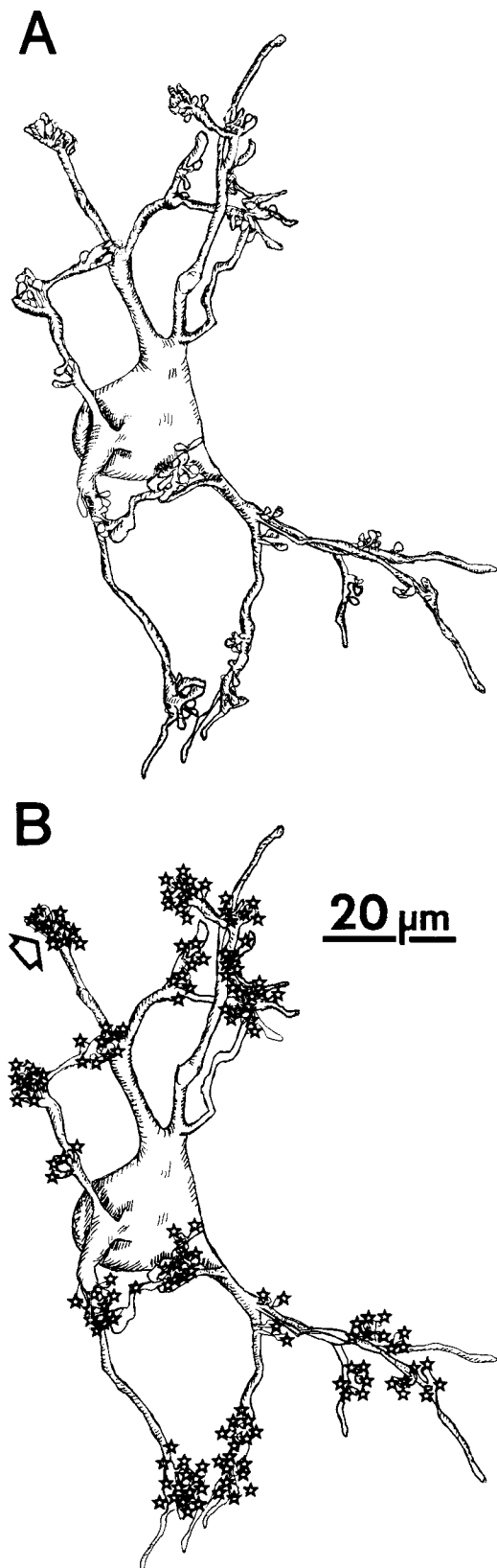


Fig. 9. Low-power reconstructions of *cell 2*. A: Reconstruction illustrating these distinctive clusters of appendages along the dendrites of *cell 2*. The axon of this cell is not shown, because it is directed rostrally and is obscured by the soma. B: Reconstruction, as in A, with the sites of synapses from retinal terminals indicated. Note that *cell 2* receives such synapses only from labeled terminals (open stars) and that these focus at regions with clusters of dendritic appendages. The open arrow refers to the area detailed in Figure 10.

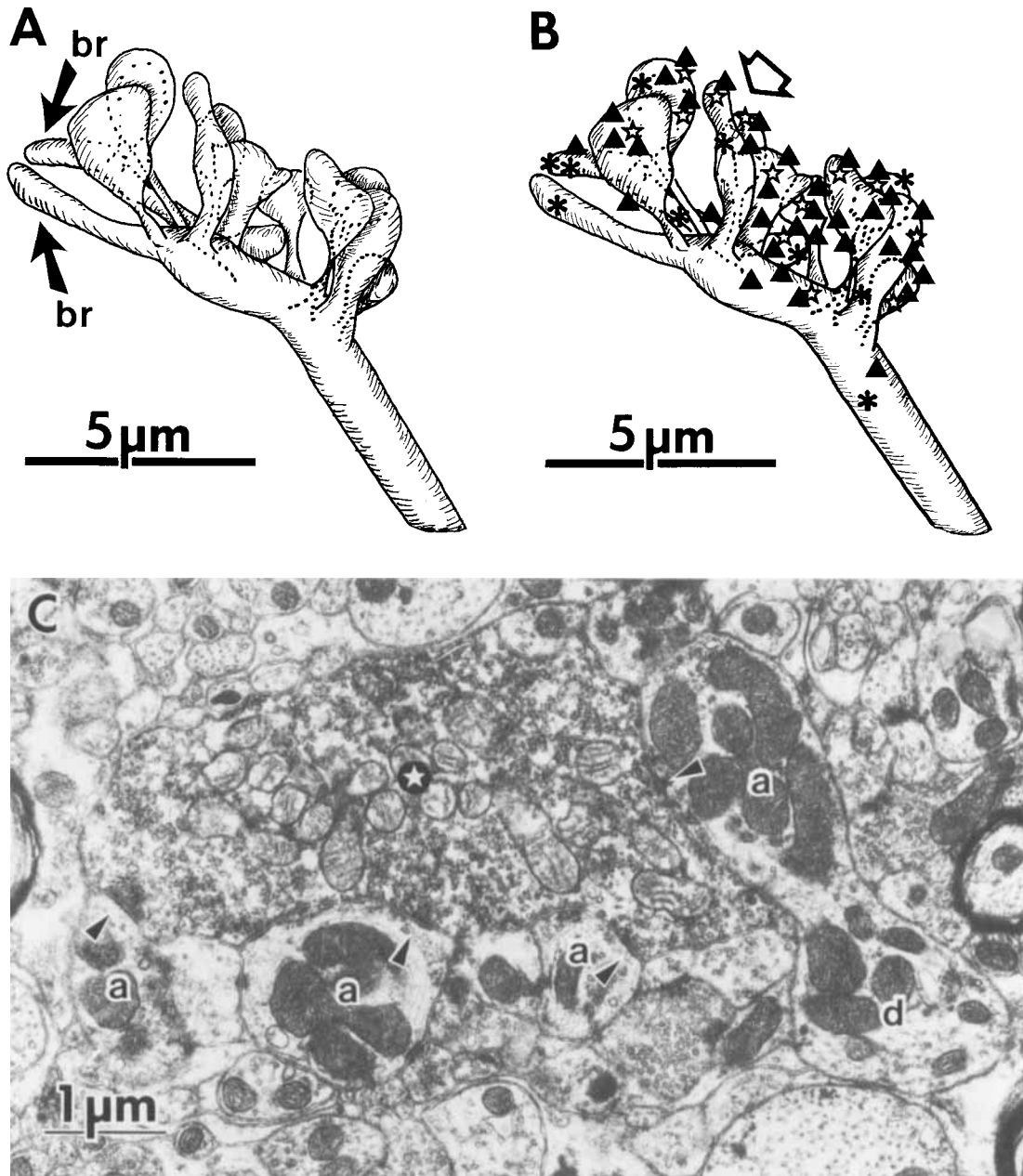


Fig. 10. High-power reconstructions and electron micrographs of *cell 2*. **A:** Detailed reconstruction of a cluster of 12 appendages emitted within a short segment of dendrite. Two fine, appendage-bearing branches (br) are also indicated. **B:** Reconstruction, as in A, illustrating all of the input to this cluster of appendages; symbols as in Figure 7. Appendages from *cell 2* receive numerous synapses, including triadic input and synapses from RSD terminals. The open arrow indicates the location of the terminal shown in C. **C:** Micrograph of a large, labeled terminal (star) contacting four appendages (a) that were reconstructed to the same *cell 2* dendrite (d).

distribution of retinal synapses ends abruptly on each dendrite and is followed by a dense innervation from RSD terminals. Synapses from F terminals tend to follow the distribution of those from retinal terminals. However, F terminals also provide the dominant input to the soma and the only synapses to the axon hillock.

Cell 4. All of the morphological features of *cell 4* suggest that it is a Y-cell. These features include the large size of its soma ($765 \mu\text{m}^2$ in cross-sectional area), which not only falls exclusively in the Y-cell range but is one of the largest cell bodies in our sample (Fig. 5), and its thick dendrites with few dendritic appendages. No cytoplasmic laminated

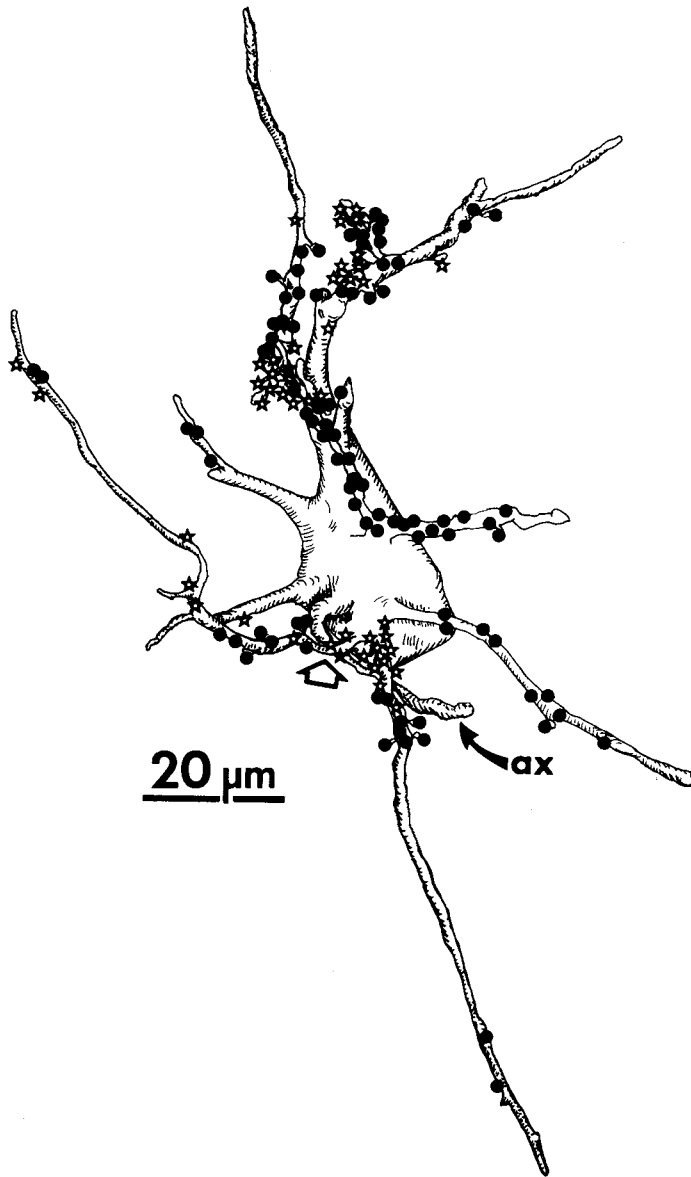


Fig. 12. Low-power reconstruction of the dendrites and axon (ax) of *cell 3* illustrating the locations of synapses from retinal terminals; symbols as in Figure 6. This cell receives convergent input from labeled and unlabeled retinal terminals. The open arrow refers to the area detailed in Figure 13.

relatively large and sparsely distributed throughout the dendritic arbor (e.g., Fig. 16). An axon emerges from the soma of *cell 4* but, because of its ventral course, it was not reconstructed beyond a limited portion of the axon hillock (Fig. 15, ax).

Cell 4 receives few synapses from the labeled axon (Fig. 15). Due to the large size of the neuron's dendritic arbor, we could not accurately determine the precise percentage of retinal synapses provided by the labeled axon. However, they represent only 12 (or 6%) of the 194 retinal synapses reconstructed on *cell 4*. Because we limited the reconstruc-

tion of five primary dendrites that did not penetrate the labeled axon's terminal arbor to within 50 μm of the cell's soma, the actual contribution is probably a much smaller percentage of the total retinal input to this cell. These dendrites almost certainly receive input from many unlabeled retinal terminals beyond those included in our reconstructions.

The 12 synapses from the labeled axon derive from 11 terminals. They are spread over the third- through sixth-order dendrites of four different dendrites and contact both shafts and appendages of these dendrites (Fig. 16A,B). These synapses from labeled terminals are more distally located on the dendritic arbor than are the bulk of the retinal synapses from unlabeled terminals (Fig. 17), and this difference in relative location is statistically significant ($P < .001$ on a chi-square test). In the zone from 5 to 90 μm from the soma of *cell 4*, only retinal synapses from unlabeled RLP terminals are found (Fig. 16C), yet this zone includes 15 retinal synapses onto primary dendrites and 151 (or 83%) of the 182 retinal synapses from unlabeled terminals. Distal to this zone, dendrites primarily receive a dense RSD terminal innervation and a limited number of synapses from RLP and F terminals. The 11 labeled retinal terminals provide their 12 synapses onto this portion of the dendritic arbor that extends over 90 μm , and typically beyond 150 μm , from the soma. Unlabeled retinal terminals also provide 31 synapses to dendrites in this zone.

Of the 12 synapses contacting *cell 4* from the labeled axon, two (or 17%) participate in synaptic triads, and six (or 50%) are located on dendritic appendages. Of the 182 synapses from unlabeled retinal terminals on the same cell, only 16 (or 9%) are members of triads and 44 (or 24%) contact dendritic appendages. These patterns do not differ statistically for labeled and unlabeled retinal terminals. Overall, then, retinal synapses on *cell 4* tend to isolate themselves on dendritic shafts, since they do not have synaptic contacts with nearby F terminals (Fig. 16D). Moreover, they are not found in synaptic glomeruli. As is shown in Table 1, labeled terminals are less frequently associated with synaptic triads on *cell 4* than is the case for the other reconstructed neurons ($P < .001$ when compared to *cells 2* and *3* and $P < .01$ when compared to *cell 1* on chi-square tests).

Figure 17 summarizes the pattern of synaptic inputs to the dendrites of *cell 4*. RSD terminals provide a dense innervation to dendrites over 80 μm from the soma, especially within the zone that receives synapses from labeled retinal terminals. As is the case for most geniculate neurons, the relative distribution of synapses from F terminals matches that of the retinal innervation, and F terminals also provide the dominant input to the soma.

Differential innervation from the labeled axon

A remarkable feature of the retinogeniculate circuitry initiated from the labeled axon is the diversity of the patterns of connectivity between the axon and its postsynaptic geniculate cells. Many examples of this are provided in our data, and more quantitative detail is given below in Retinal Terminal Morphometry. Figure 18 summarizes a particularly illuminating feature of this diversity by showing the location of synapses from labeled retinal terminals relative to the cell bodies of *cells 1-4*. The varying zones of synapses from labeled terminals suggest that the single, labeled axon contacts different dendritic regions from each of its postsyn-

A

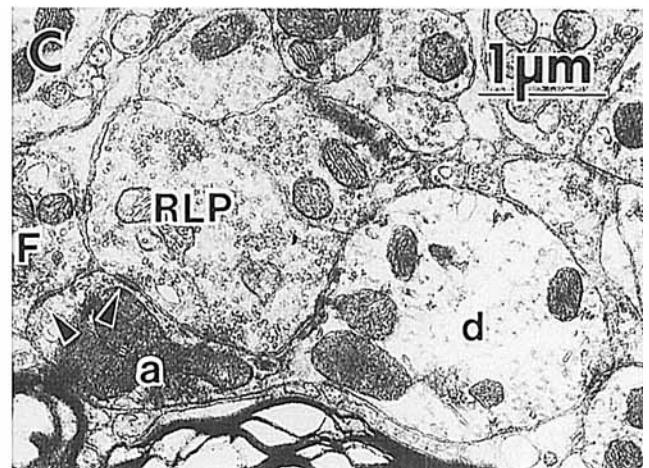
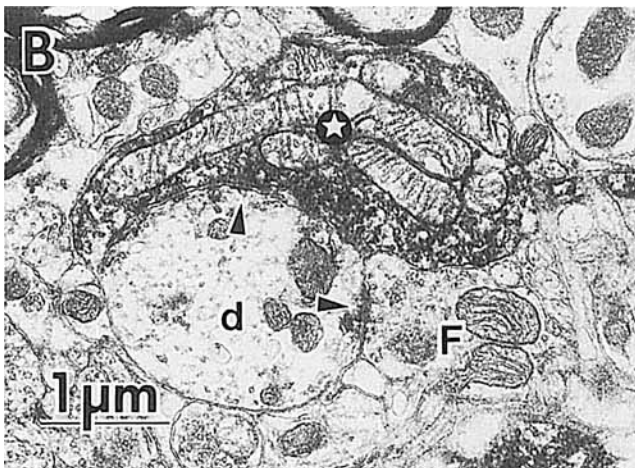
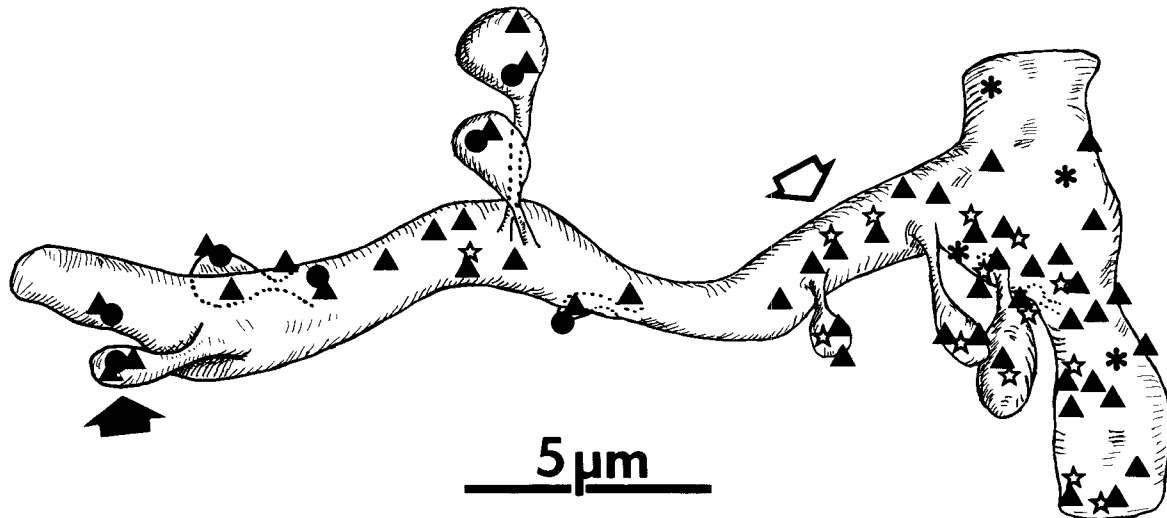


Fig. 13. High-power reconstruction and electron micrographs of *cell 3*. A: Detailed reconstruction of a major dendritic branch point illustrating numerous appendages in this region and the inputs to these structures; symbols as in Figure 7. The arrows indicate synapses shown in B (open arrow, synapse from labeled terminal) and C (closed arrow, synapse from unlabeled RLP terminal), respectively. B: Micrograph of a labeled terminal (star) and an F terminal synapsing directly on the dendritic shaft (d). C: Micrograph of an unlabeled RLP terminal and an F terminal contacting an appendage (a) emitted from a dendrite (d) of *cell 3*.

aptic geniculate cells. These differences in innervation pattern are statistically significant for each pairwise comparison of cells ($P < .001$ between *cell 4* and each of the other cells, $P < .001$ between *cell 2* and *cell 1*, $P < .01$ between *cell 2* and *cell 3*, $P < .05$ between *cell 1* and *cell 3*).

Electrotonic distances of synaptic locations

All of the above-mentioned assessments of synaptic location on *cells 1–4* refer simply to anatomical distances from the somata. However, the electrotonic distance of each synapse from the soma is a more relevant indicator of its efficacy (Jack et al., '75). By employing a simple algorithm and adopting certain assumptions, we estimated the relative electrotonic distance for each synapse (see Materials

and Methods). We found a strong linear relationship ($r > .99$) between the relative electrotonic distances and the measured anatomical distances for synapses from each population of terminal types on each of the cells postsynaptic to the labeled axon (Fig. 19). This relationship is neither trivial nor tautological since there is no reason to assume a geometric constraint on dendritic morphology that would produce this observation. For example, dendrites that arborize with branches whose diameters are equivalent to that of the parent dendrite will not exhibit a linear relationship between anatomical and electrotonic distance from the soma.

Previously, we noted that, for each of *cells 1–4*, synapses from labeled terminals occur at roughly equal anatomical distances from the soma, even when the terminals inner-

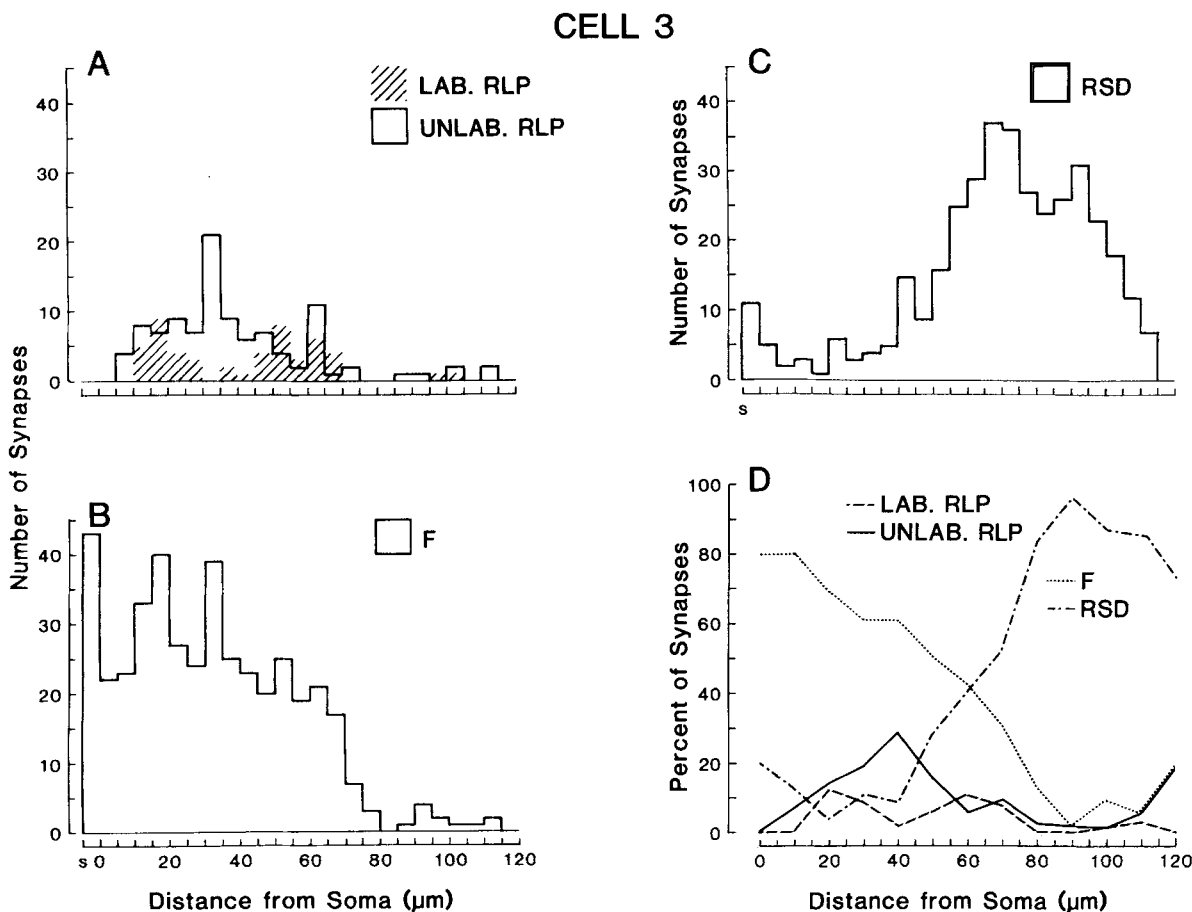


Fig. 14. Graphs showing distributions of synapses from different terminal populations along the dendrites of cell 3; conventions as in Figure 8. Note that synapses from RSD terminals predominate in the region beyond 60 μm from the soma while the distribution of synapses from F terminals mirrors that from both labeled and unlabeled RLP terminals to the more proximal dendrites.

vate different dendrites of the same cell. However, these distances vary among the cells. From the above, it follows that these synapses are located at roughly equivalent electrotonic distances from the somata of cells 1-4. This suggests that the efficacy of synapses derived from the labeled axon, even if on different dendritic processes, will be equal relative to soma. Of course, these conclusions require that the assumptions underlying cable theory be met for these cells. In particular, our conclusions become invalid if the dendrites exhibit nonuniform specific membrane resistance and respond nonlinearly to postsynaptic potentials with such behavior as voltage-dependent conductance changes.

Relationship of postsynaptic neurons to the axon's terminal field

Since phenomena such as conduction failure may occur in axonal terminal arbors (for review, see Parnas, '79), we examined whether there was any relationship between the branching pattern of the labeled axon and the geniculate cells it innervates. If so, this might serve as a morphological substrate for the exclusion of active inputs to specific neurons under certain physiological conditions. Nevertheless,

there is no obvious relationship between the labeled terminals innervating different postsynaptic cells and the axonal branches from which these terminals derive. We often found that successive terminals along the same branch of the labeled axon contact different neurons. However, although neighboring terminals may contact different geniculate cells, synapses from single terminals are restricted to a single postsynaptic projection neuron. Only four of the 113 labeled terminals that contact our reconstructed neurons form synapses onto more than one reconstructed postsynaptic cell (Fig. 20B). Here, however, we discount as potential postsynaptic neurons the F terminals that are commonly contacted by labeled retinal terminals and originate from the dendrites of local circuit neurons.

As stated previously, many labeled terminals are boutons *en passant* along a myelinated portion of the axon. Other *en passant* terminals exhibit myelinated preterminal axon segments and unmyelinated extents of axon directed distally from the terminal. Still others have solely unmyelinated preterminal segments either on both ends or on one if the bouton is the terminus of an axonal branch. These findings further suggest that the terminal arbor has a var-

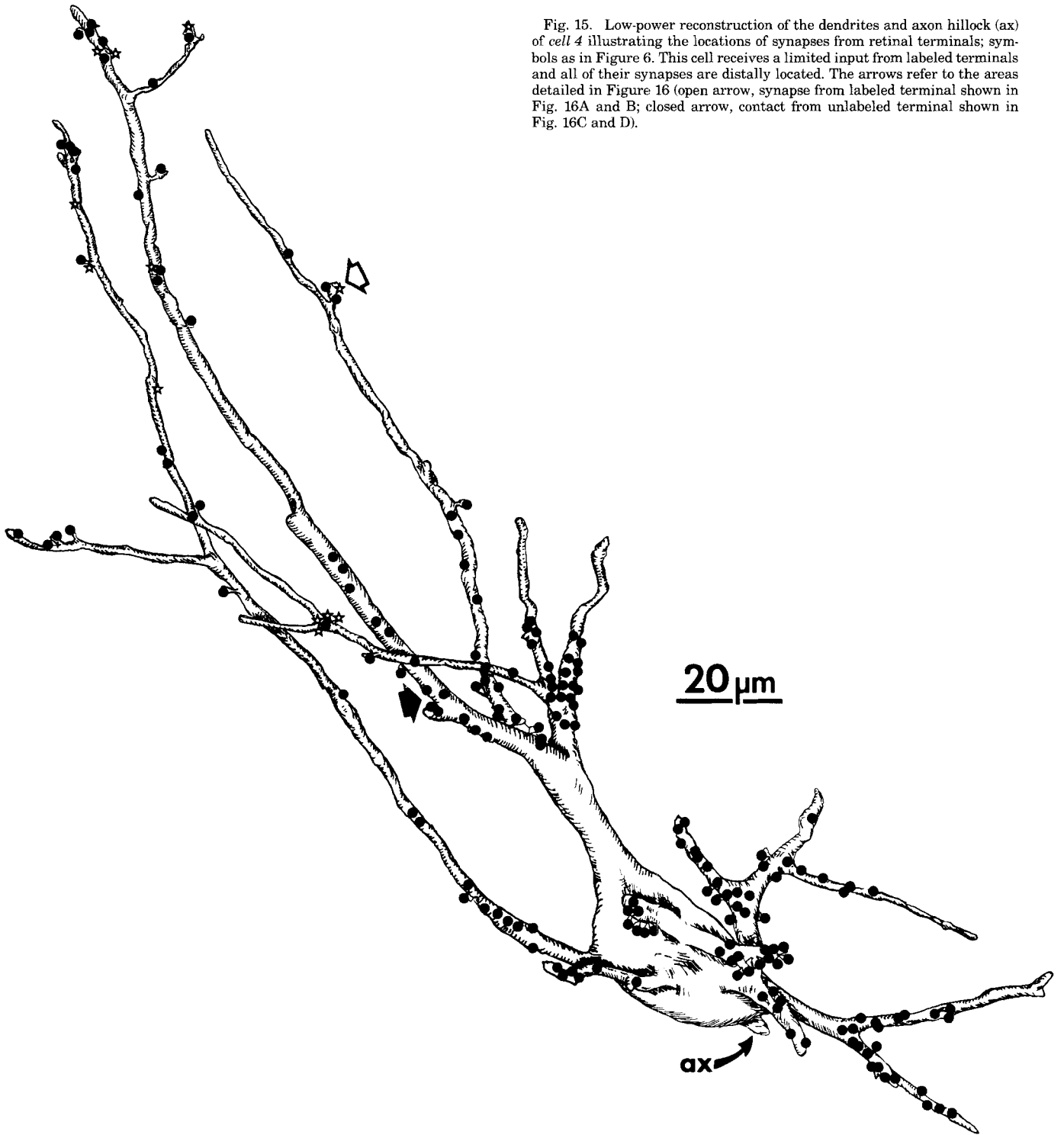


Fig. 15. Low-power reconstruction of the dendrites and axon hillock (ax) of *cell 4* illustrating the locations of synapses from retinal terminals; symbols as in Figure 6. This cell receives a limited input from labeled terminals and all of their synapses are distally located. The arrows refer to the areas detailed in Figure 16 (open arrow, synapse from labeled terminal shown in Fig. 16A and B; closed arrow, contact from unlabeled terminal shown in Fig. 16C and D).

ied myelination pattern, the physiological importance of which is open to question.

Neurons not innervated by the labeled axon in its terminal arbor

We sought to characterize the selectivity of connections formed by the labeled axon in the ventral portion of its terminal arbor. One measure of this selectivity is the number of neurons not receiving inputs from the labeled axon despite being physically in a position to receive such inputs. We therefore determined how many neurons are located within the ventral portion of the labeled axon's arbor or had dendrites that penetrate this region. To do this, we analyzed low-magnification electron micrographs of every tenth section through the series to reconstruct the position of every soma in the region relative to the terminal arbor and to produce a two-dimensional map of this reconstruction (Fig. 4).

Overall, there are 43 neurons in the ventral region of the labeled axon's terminal arbor. This includes the cell bodies and proximal dendritic segments of 31 neurons as well as portions of the dendritic arbors of 12 additional neurons (Fig. 4). As noted above, the labeled axon provides synapses to the dendritic shafts and appendages of four of these 43 neurons. However, this analysis accounts for only 113 (or 73%) of the 155 labeled terminals. The postsynaptic targets for the remaining 42 terminals are unknown.

The 39 neurons not innervated by the labeled axon display a wide variety of morphological features. Although we limited the reconstruction of geniculate cells that do not receive synapses from labeled retinal terminals, many clearly have small cell bodies whose sizes fall entirely within the X-cell range (Fig. 5). Furthermore, 20 of the 39 neurons contain cytoplasmic laminated bodies, a feature thought to mark X-cells (LeVay and Ferster, '77). Finally, a number of these neurons possess features characteristic of most geniculate X-cells, including dendrites that exhibit abundant appendages and that are the postsynaptic elements in triads. In summary, many of the above-mentioned 39 cells have the morphological characteristics of X-cells and might be considered as likely postsynaptic partners for a retinal X-cell axon.

Retinal terminal morphometry

We used serial sections to reconstruct and measure the volumes of the 155 labeled terminals and of 50 randomly selected, unlabeled retinal terminals from the same ventral region of the labeled axon's terminal arbor (Fig. 20). The volumes of the unlabeled RLP terminals range from $1.9 \mu\text{m}^3$ to $78.1 \mu\text{m}^3$. Likewise, the labeled terminals span roughly the same range with volumes between $0.2 \mu\text{m}^3$ and $56.9 \mu\text{m}^3$. There is no statistically significant difference between these distributions of terminal volume ($P > .1$), indicating that a single axon produces terminals with sizes that span the entire size range of retinal terminals (see also Robson and Mason, '79). Since the 50 unlabeled terminals are likely to include many from Y-cell axons, there is therefore no evidence for dramatic differences in terminal volume between X- and Y-cell axons.

Interestingly, different sizes of synaptic terminals from the injected axon segregate onto different postsynaptic neurons. Figure 20B shows the size distribution of labeled retinal terminals on *cells 1-4*. *Cells 1, 3, and 4* receive nearly all (> 95%) of their input from labeled terminals that are less than $20 \mu\text{m}^3$ in volume. While *cell 2* receives

synapses from labeled terminals of this size (e.g., Fig. 3), 13 (or 22%) of its 59 retinal terminals are larger (e.g., Fig. 10), and this includes 13 (or 72%) of the 18 total labeled terminals greater than $20 \mu\text{m}^3$ in volume. The tendency for larger labeled terminals to contact *cell 2* is statistically significant ($P < .001$ for each pairwise comparison between *cell 2* and *cells 1, 3, and 4*). Moreover, two of the larger terminals that contact dendritic appendages on *cells 3 and 4* also provide three and four synapses each to *cell 2*. These represent two of only four cases in which a single, labeled terminal provides synapses to two of the reconstructed neurons. Of the five larger terminals not found to contact *cell 2*, four synapse on processes that we were unable to reconstruct to any of the four postsynaptic cells, although these might conceivably contact *cell 2* despite our failure to demonstrate this (see Discussion), and one contacts *cell 3* exclusively.

Each of the labeled terminals makes between one and 28 synapses onto F terminals, dendritic appendages, and/or dendritic shafts. Figure 21 shows that the number of synapses formed by each of these terminals is closely linked to the terminal volume ($r = .86$; $P < .001$). Furthermore, a close correlation exists between the number of synapses formed by each labeled terminal onto F terminals and the number formed onto dendritic appendages and shafts ($r = .98$; $P < .001$). It follows from these relationships that the number of synapses per labeled retinal terminal should differ among *cells 1-4* (Fig. 21), because the distribution of terminal volumes differs among these postsynaptic neurons (Fig. 20B). *Cells 1, 3, and 4* receive inputs from labeled terminals that provide one to 14 synapses, with a mean of 3.2 synapses per terminal. *Cell 2* receives inputs from labeled retinal terminals that provide one to 28 synapses, with a mean of 7.8 synapses per terminal. This distribution for *cell 2* differs significantly from that for *cells 1, 3, and 4* ($P < .001$).

DISCUSSION

We injected HRP into a single retinal X-cell axon in the optic tract, thereby labeling its entire terminal arbor in the lateral geniculate nucleus. We then used electron microscopic methods to reconstruct those geniculate neurons receiving synaptic contacts from labeled terminals in a proscribed portion of the labeled axon's terminal arbor. We identified an exquisite selectivity in the pattern of synaptic contacts formed by this portion of the terminal arbor. Only four geniculate neurons are postsynaptic to terminals from the reconstructed portion of the labeled axon, and this represents less than 10% of the cells available on the basis of their location relative to that of the axon's terminal arbor. Furthermore, the labeled terminals provide synapses to specific regions of each postsynaptic geniculate neuron's dendritic arbor. We also discovered a surprising degree of heterogeneity in the morphology and synaptic relationships of the postsynaptic cells. These cells differ with regard to soma size, dendritic morphology, the pattern of their synaptic inputs (from both labeled retinal terminals as well as unlabeled terminals from various sources), and the complexity of any synaptic glomeruli with which they are associated. Of the four identified cells postsynaptic to the labeled axon, three are presumed to be X-cells, as expected, but one seems to be a Y-cell that receives a scant innervation from that axon.

Evaluation of the method

We have chosen to reconstruct with the electron micro-

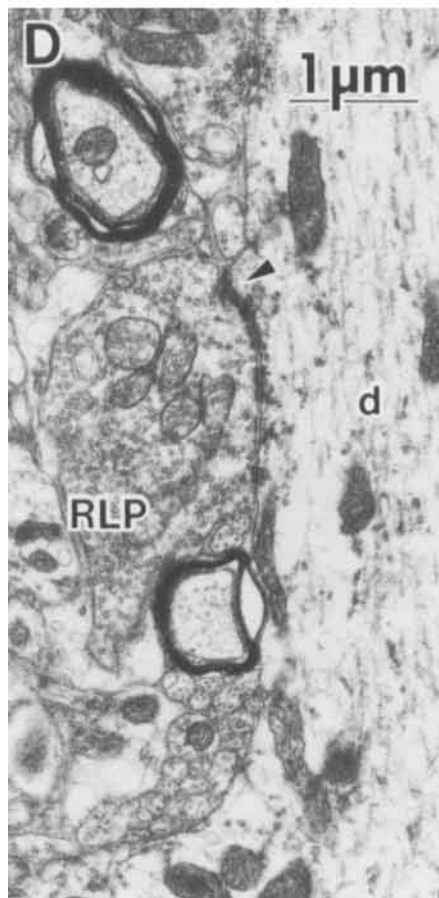
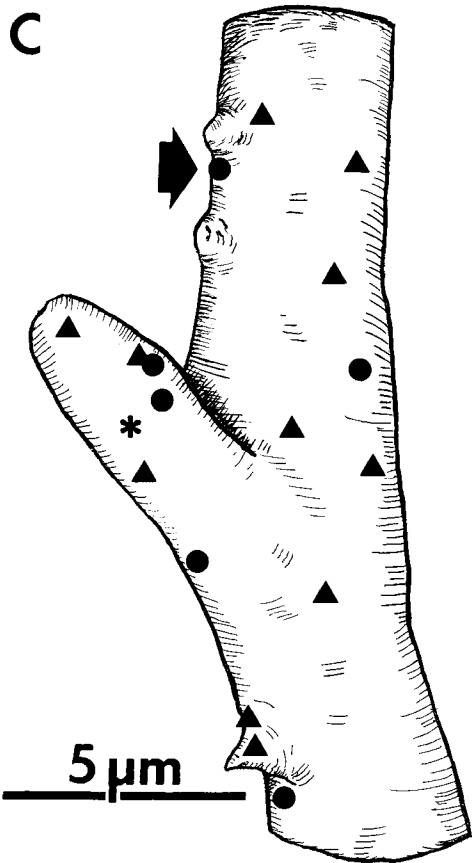
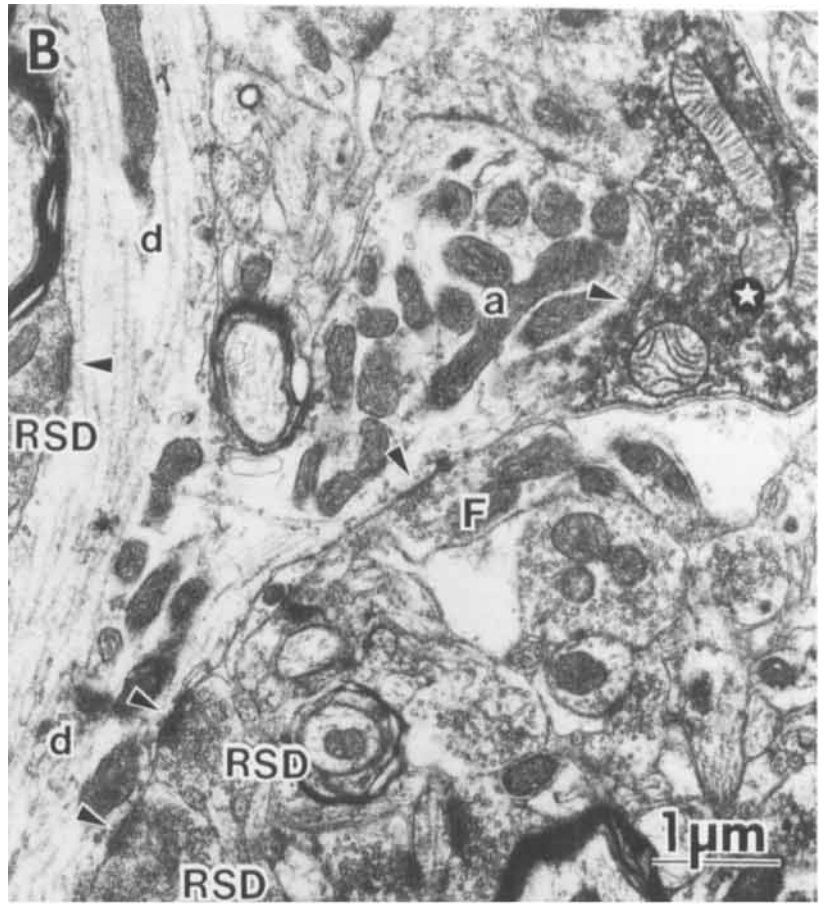
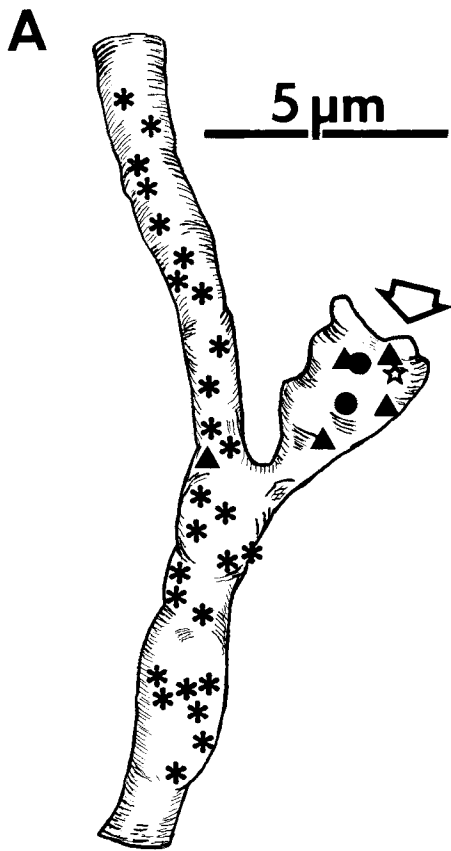


Figure 16

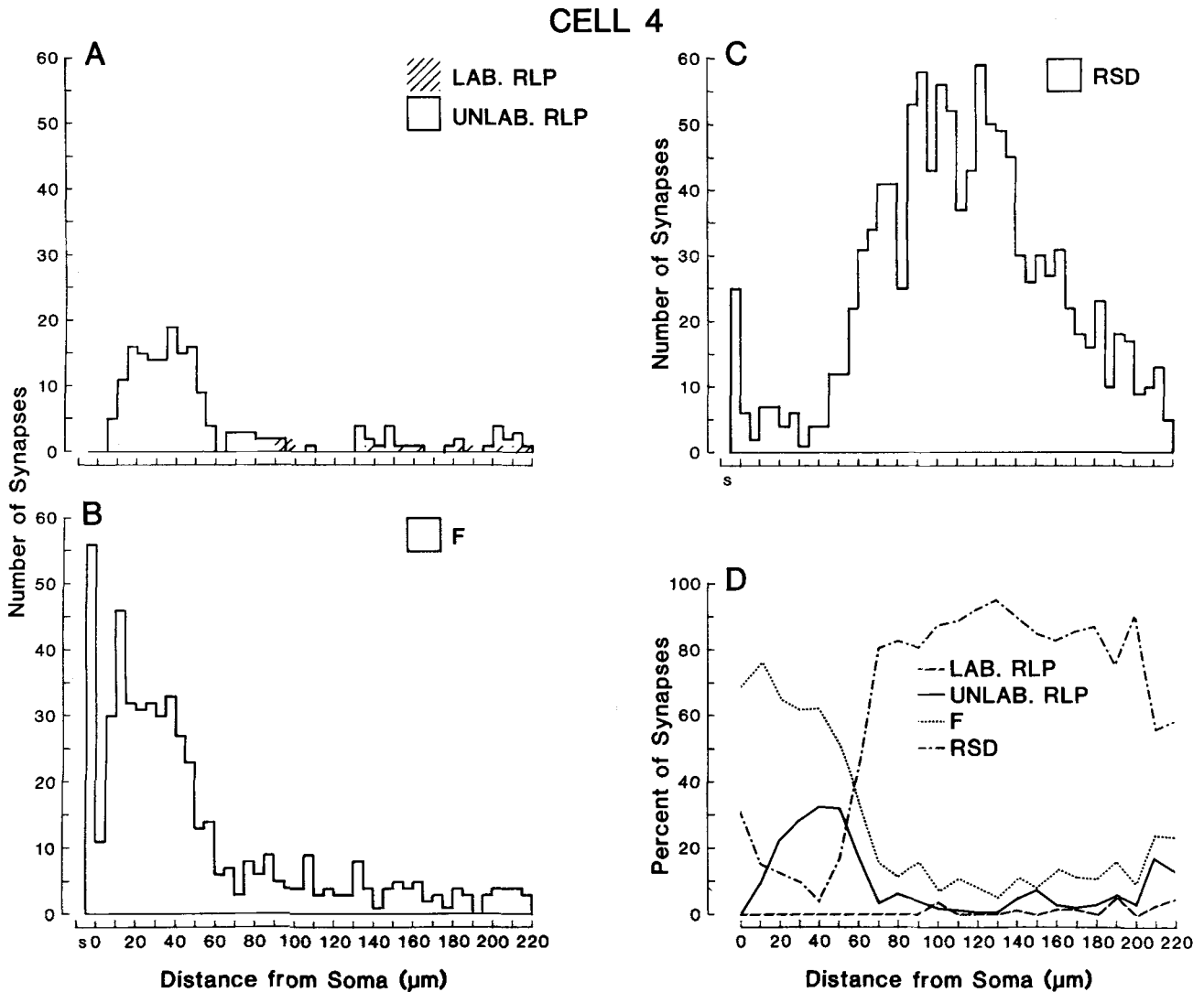


Fig. 16. High-power reconstructions and electron micrographs of cell 4. A: Detailed reconstruction of a large appendage, located 136 μm from the soma, that receives synapses from both labeled and unlabeled retinal terminals; symbols as in Figure 7. The adjacent dendritic shaft receives a dense innervation from RSD terminals. The open arrow indicates a synapse from the labeled terminal shown in B. B: Micrograph of a labeled terminal (star) synapsing on a large appendage (a) in the vicinity of synapses from

other terminals that primarily contact the parent dendrite (d). C: Detailed reconstruction of a branch point located 60 μm from the soma receiving retinal input only from unlabeled terminals that generally do not participate in triads. The closed arrow indicates a synapse from the unlabeled RLP terminal shown in D. D: Micrograph of an unlabeled RLP terminal contacting a dendrite (d) in isolation from other synapses.

scope the postsynaptic targets of an HRP-labeled axon, because this method permits the elucidation of detailed synaptic circuitry related to single afferent axons. The discovery of selectivity in the number of neurons contacted in light of the diversity in the synaptic relationships formed

by the labeled axon on these neurons is particularly interesting and unexpected. However, our method does have a number of limitations, four of which are described below.

First and most serious, the method is labor-intensive and time consuming. The surprising degree of heterogeneity seen in the circuits formed by the single axon highlights the need for more data before the present results can be generalized to all retinogeniculate circuitry in cats. This will require similar studies of several more retinogeniculate axons from X-cells plus several from Y-cells. While it will never be practical to obtain such analyses for large populations of afferent axons, we believe that reasonable conclusions can be drawn from a more limited and practical sample.

Second, while it might be useful to reconstruct the entire dendritic arbor of each geniculate cell contacted by the labeled axon, we did not do so. We generally stopped our reconstructions just beyond the point at which dendritic

Fig. 16. High-power reconstructions and electron micrographs of cell 4. A: Detailed reconstruction of a large appendage, located 136 μm from the soma, that receives synapses from both labeled and unlabeled retinal terminals; symbols as in Figure 7. The adjacent dendritic shaft receives a dense innervation from RSD terminals. The open arrow indicates a synapse from the labeled terminal shown in B. B: Micrograph of a labeled terminal (star) synapsing on a large appendage (a) in the vicinity of synapses from other terminals that primarily contact the parent dendrite (d). C: Detailed reconstruction of a branch point located 60 μm from the soma receiving retinal input only from unlabeled terminals that generally do not participate in triads. The closed arrow indicates a synapse from the unlabeled RLP terminal shown in D. D: Micrograph of an unlabeled RLP terminal contacting a dendrite (d) in isolation from other synapses.

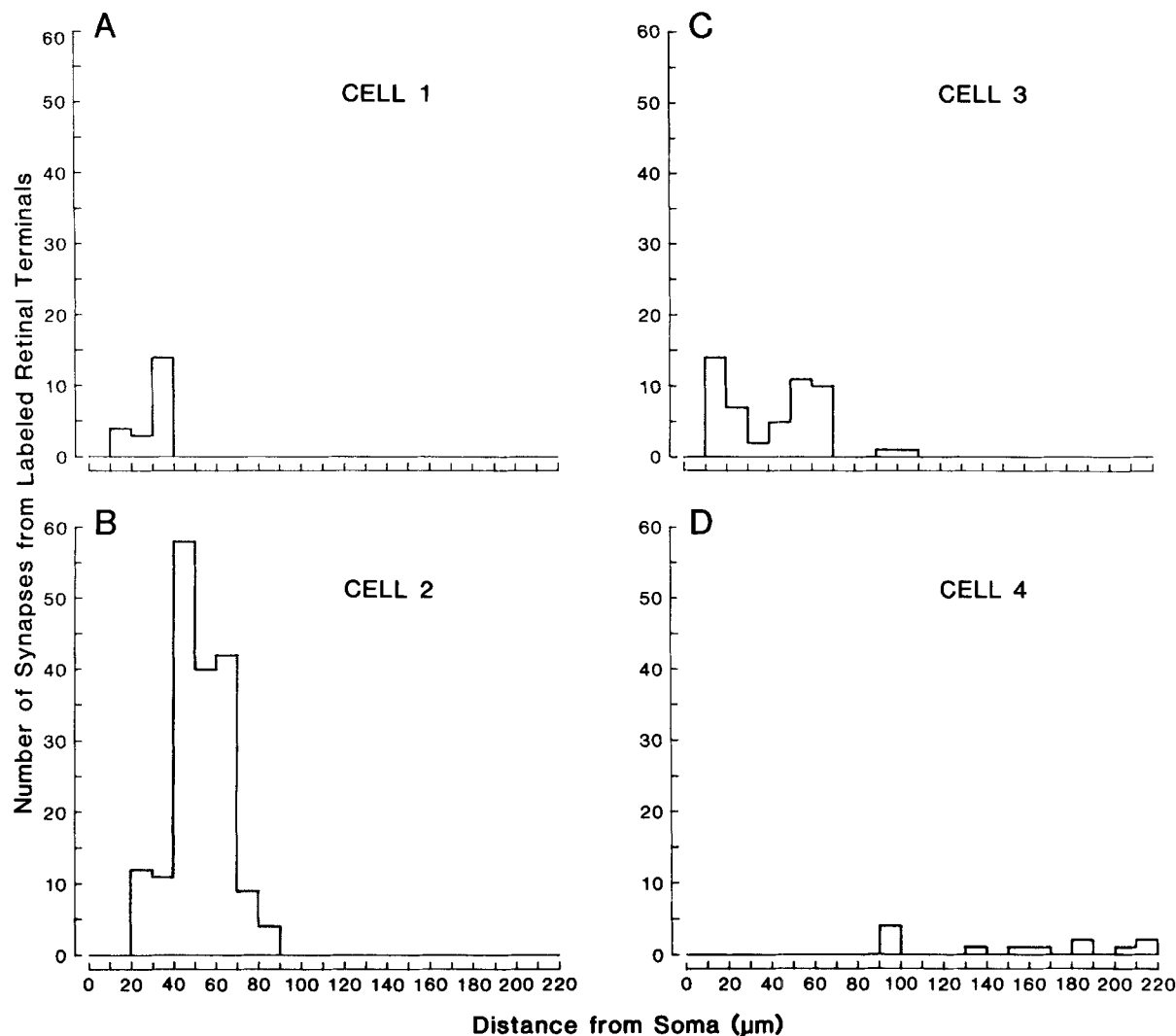


Fig. 18. Graphs showing distributions of synapses from labeled retinal terminals onto the dendrites of each of the four reconstructed neurons. These synapses onto *cells 1, 2, and 3* are typically located within 100 μm of their respective somata while those onto *cell 4* are generally scarce and located over 100 μm from its soma. The greatest number of synapses from labeled terminals are focused onto *cell 2*, which is the only neuron of those reconstructed to receive all of its retinal input from the injected axon.

segments leave the region of the labeled terminal arbor, and probably as a result, we did not relate every labeled terminal to a specific postsynaptic neuron. Nevertheless, we could assign 113 (or 73%) of the 155 labeled terminals to four postsynaptic neurons. The remaining 42 terminals are concentrated on segments of a few dendrites, mostly on dendritic appendages that are postsynaptic elements in triads. Since the morphological features of synaptic circuitry evident from these terminals are thus rather similar to those described for the other 113 terminals, our conclusions would not be substantively different had they been based on an assignment of every labeled terminal to a specific postsynaptic cell. It is also possible, and indeed likely, that the dendritic segments contacted by many of the unassigned 42 terminals belong to portions of the four identified

postsynaptic neurons that coursed out of the axon's terminal arbor.

Third, because our reconstructions of unlabeled postsynaptic targets could not include extremely thin processes, we could not identify the dendrite of origin for every process postsynaptic to labeled terminals. Processes with a diameter approaching the thickness of a thin section (roughly 0.08 μm) are generally untraceable, and some of the postsynaptic targets of labeled terminals were initially followed to such fine processes. For example, we were unable to reconstruct the postsynaptic F terminals to the dendrites or somata of their origin, because these F terminals are appended to their parent dendrites by extremely fine process (Famiglietti and Peters, '72; Hamos et al., '85). We undertook the present study because most postsynaptic

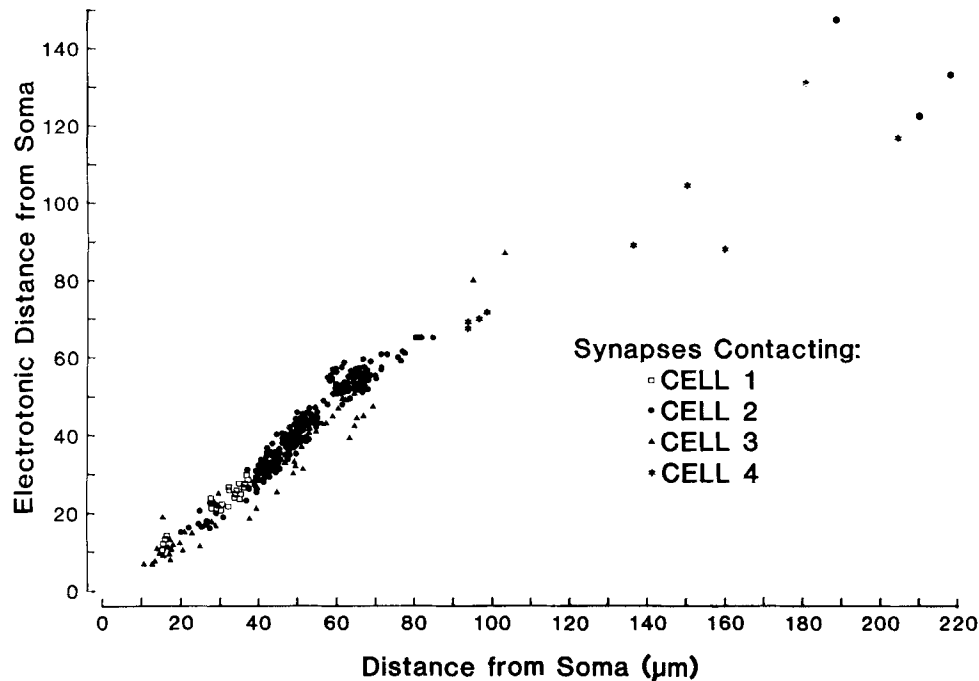


Fig. 19. Scatter plot of the measured distances between the soma and points on the dendrites receiving synapses from labeled terminals vs. the relative electrotonic distances calculated from considerations of dendritic morphology (see text). Because the ordinate values are relative, they signify no units. For the inputs from labeled terminals onto each of the four reconstructed neurons, there is a linear relationship between these variables suggesting that the measure of actual distances along dendrites provides valid functional measurements to describe the locations of synapses onto these geniculate cells. A scatter plot with a similar linear relationship can be generated for synapses from each terminal variety impinging on the four reconstructed neurons.

dendritic appendages on geniculate neurons connect to their parent dendritic shafts with processes large enough to be traced.

Fourth, we have assumed that the entire arbor of the injected X retinogeniculate axon is labeled. For the following reasons we believe this assumption to be valid: (1) The arbor is typical of many other labeled X-cell arbors studied at the light microscopic level (Sur and Sherman, '82; Bowling and Michael, '84). This includes such parameters as overall geometry and the number of boutons. (2) All of the preterminal endings are boutons, and if the labeled incompletely penetrated the arbor, we would expect fading of the label prior to many boutons. (3) The label was uniformly dense throughout the arbor. This is typical for well-filled retinogeniculate X-cell arbors, which tend to display limited branching. Variability in label is characteristic of incompletely filled axon arbors, which often display widespread preterminal branching. This may occasionally be seen in retinogeniculate Y-cell arbors (unpublished observations), geniculocortical axon arbors (Humphrey et al., '85a,b), or intracortical axon arbors (McGuire et al., '84). (4) Finally, since *cell 2* receives all of its retinal input from the labeled axon, the portion of the arbor innervating it must be completely labeled, and a number of separate preterminal branches give rise to the retinal terminals innervating this cell.

Are the reconstructed postsynaptic neurons projection neurons or interneurons?

An initial issue that cannot be unambiguously resolved concerns the identity of the reconstructed cells postsynaptic

to the labeled axon; i.e., which of these are projection neurons and which are interneurons since both neuron types are innervated directly by optic tract axons (Dubin and Cleland, '77; Hamos et al., '85)? Although all four reconstructed neurons have axons, this is not a diagnostic feature of projection neurons since geniculate interneurons have locally ramifying myelinated axons (Hamos et al., '85). Once again, the discussion below excludes the postsynaptic F terminals, most or all of which certainly derive from interneurons (Famiglietti and Peters, '72; Hamos et al., '85).

On the basis of soma size and dendritic morphology, we are confident that *cells 3* and *4* are projection neurons (Famiglietti and Peters, '72; LeVay and Ferster, '77, '79; Friedlander et al., '81; Fitzpatrick et al., '84; Hamos et al., '85). While *cell 1* is small enough to be an interneuron, we believe it to be a projection neuron for the following reasons: (1) Within the reconstructed region, its dendrites lack the complex appendages associated with interneurons (Famiglietti and Peters, '72; LeVay and Ferster, '77, '79; Friedlander et al., '81; Fitzpatrick et al., '84; Hamos et al., '85); (2) it possesses a cytoplasmic laminated body, a feature that is only associated with a subpopulation of projection neurons (LeVay and Ferster, '77); and (3) projection neurons have been described with somata as small as that of *cell 1* (Friedlander et al., '81; Fitzpatrick et al., '84). Only *cell 2* is difficult to assign as a projection neuron or an interneuron. Although the cross-sectional area of its soma falls just below the upper limit of the range suggested for interneurons (LeVay and Ferster, '79; Sterling and Davis, '80; Fitzpatrick et al., '84), its clusters of dendritic appendages are not

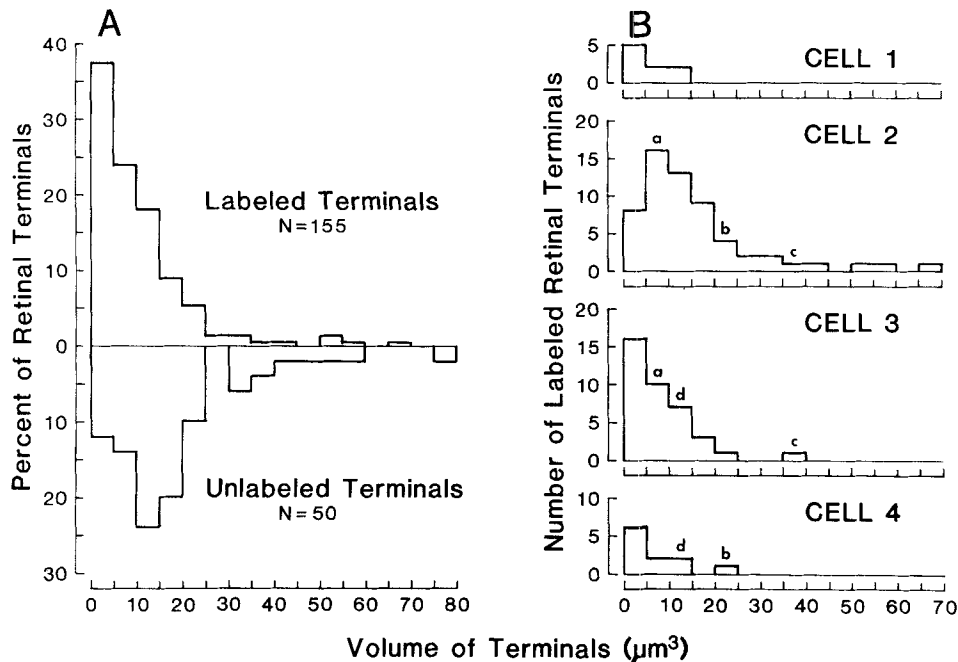


Fig. 20. Size distributions of retinal terminals. A: Comparison of labeled and unlabeled terminals. The upper histogram represents the population of labeled terminals with each bin indicating the relative percentage of labeled terminals ($N = 155$). The lower histogram is an analogous representation of a population of randomly selected, unlabeled RLP terminals ($N = 50$). The distribution of the sizes from labeled terminals is similar to that of the unlabeled RLP terminals, and these distributions span the same range. The upper histogram is slightly skewed to the left, presumably due to the enhanced ability to detect small retinal terminals with the HRP label. Unlabeled terminals of a similar size ($< 2 \mu\text{m}^3$) are virtually impossible to detect. B: Terminal size distributions of labeled retinal terminals providing synapses to each of the four reconstructed neurons. Note that nearly all of the large, labeled terminals ($> 20 \mu\text{m}^3$) contact *cell 2*. Also indicated are the sizes and postsynaptic neurons of the four terminals (*a*, *b*, *c*, and *d*) that contact more than one cell.

similar to the complex appendages associated with interneurons (Guillery, '66; Famiglietti and Peters, '72; Hamos et al., '85). Moreover, dendritic appendages are strictly postsynaptic for *cell 2*, while processes appended to the dendrites of interneurons are the source of pre- and postsynaptic F terminals (Famiglietti and Peters, '72; Hamos et al., '85). Indeed, the dendritic appendages of this cell are typical of those described for relay X-cells (Friedlander et al., '81; Wilson et al., '84). These observations of dendritic morphology and synaptology thus suggest that *cell 2* is a projection neuron. Nonetheless, when coupled with its lack of a cytoplasmic body, its relatively small soma suggests an interneuronal identity (LeVay and Ferster, '77; but see Fitzpatrick et al., '84). On balance, we suspect that all of the four cells postsynaptic to the labeled retinal axon are projection neurons, but this conclusion is most uncertain for *cell 2*.

Diversity of geniculate circuits related to the labeled axon

As noted above, the morphological features of the four geniculate neurons shown to receive synaptic contacts from the labeled axon are heterogeneous. While three of the neurons appear to be X-cells, their morphological features are quite different from one another. The fourth postsynaptic neuron has the characteristics of a Y-cell. Thus four neurons with variable morphology and synaptology are innervated by a portion of the single, labeled retinogeniculate axon.

Dendritic morphology of the postsynaptic cells. The dendritic heterogeneity of the three postsynaptic X-cells is consistent with the findings of Friedlander et al. ('81), who noted that geniculate X-cells seem to display considerable morphological heterogeneity, particularly when compared to the limited morphological diversity of Y-cells. Using Guillery's ('66) classification scheme, Friedlander et al. ('81) found that nearly all Y-cells are *class 1* cells, but X-cells include *class 2* cells, *class 3* cells, and various types of unclassified cells. While nearly all Y-cells have fairly smooth, cruciate dendrites with few appendages, X-cells display a wide range of dendritic features, including fairly smooth, straight dendrites, extensively curved dendrites, varicose and beaded dendrites, and dendrites with numerous appendages. Even appendage morphology differs among X-cells. These appendages can be simple or clustered, closely attached to the dendritic shaft or appended to it by long processes, and concentrated at dendritic branch points or distributed all along the dendrites (Friedlander et al., '81; Weller and Humphrey, '85).

Such morphological heterogeneity might have physiological correlates. Recent experiments by Mastronarde ('81, '83, '85) suggest that geniculate X-cells may be further categorized on the basis of their response properties to flashing stimuli, the number of retinal neurons that innervate them, their conduction velocity, and the probability of their response to optic chiasm stimulation (see also Humphrey and Weller, '85). Moreover, geniculate X-cells as a neuronal class are more variable in their passive electrical

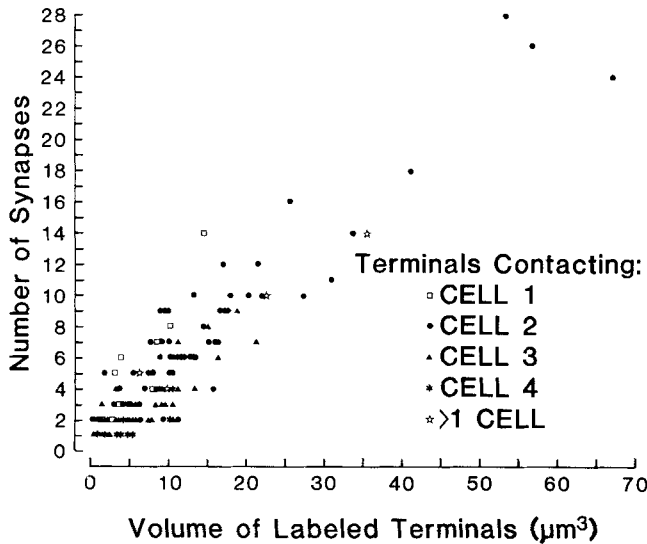


Fig. 21. Scatter plot of the size of labeled terminals versus the total number of synapses that they provide (to dendritic shafts and appendages and to F terminals). Terminals contacting *cell 2* tend both to be large and to provide numerous synapses as befits their participation in complex glomerular arrangements. Terminals contacting *cell 4* are typically small and provide only the single synapse to a distal portion of this cell; they rarely participate in synaptic triads. Those terminals that synapse on more than one cell (open stars) are identical to the four terminals indicated in Figure 20B.

properties than are geniculate Y-cells (Bloomfield et al., '85). Because a single axon contacts such a range of X-cell types in our reconstructions, we conclude that the morphological heterogeneity seen among geniculate X-cells (Friedlander et al., '81; Weller and Humphrey, '85) does not necessarily reflect inputs from separate subclasses of retinogeniculate X-cell axons. Rather, this heterogeneity reflects the reorganization of information carried by an individual afferent axon to a diverse population of geniculate X-cells.

Patterns of synaptic input. A major difference among the four postsynaptic geniculate cells relates to their patterns of synaptic input. Even if *cell 4* is excluded from this analysis because of its possible status as a Y-cell, which already implies an obvious difference in synaptic inputs from that seen for X-cells (Wilson et al., '84), surprising differences still exist for the postsynaptic X-cells. *Cells 1-3* vary widely in both the absolute number of synapses from labeled terminals (21 for *cell 1* to 176 for *cell 2*) as well as the relative percentage of retinal synapses these represent (33% for *cell 3* to 100% for *cell 2*).

Other differences among these X-cells are evident in the overall patterns of synaptic inputs within the proximal dendritic arbors that we reconstructed. *Cell 1* receives only 224 synapses vs. 856 for *cell 2* and 952 for *cell 3*. Furthermore, these cells differ greatly with respect to the distribution of synapses on their dendrites: *cell 2* receives most of its input in the vicinity of clusters of dendritic appendages, each of which is a postsynaptic element in complex synaptic glomeruli; *cells 1* and *3* show no such focus of inputs largely limited to dendritic appendages and are postsynaptic to considerably simpler synaptic glomeruli or solely to synaptic triads.

A final point of diversity is the differential distribution with respect to the sizes of labeled terminals that contact these X-cells. Robson and Mason ('79) first appreciated that single retinogeniculate axons produce synaptic terminals of diverse sizes and shapes that relate to different patterns of connectivity. However, they could not determine from their material "whether or not these various arrangements relate to the same or to different postsynaptic neurons" (Robson and Mason, '79). This point was reiterated by Rapisardi and Miles ('84), who wondered if individual geniculate neurons receive synapses both from retinal terminals involved in complex synaptic arrangements (the "high triad RTs" of these authors) as well as from retinal terminals that engage in simpler synaptic circuits ("low triads RTs"). Our data clearly show that the variability in the size of retinal terminals and the associated synaptic circuitry is directly related to variability in somatic and dendritic morphology and in patterns of synaptic innervation among the different postsynaptic neurons. The relatively few large terminals from the labeled axon concentrate their inputs onto *cell 2*, presumably because the larger terminals are needed to support more synapses for the complex synaptic glomeruli that are characteristic of *cell 2*. Moreover, all of the retinal terminals innervating *cell 2* are "high triad RTs" in the terminology of Rapisardi and Miles ('84), while those contacting *cells 1, 3, and 4* are "low triad RTs."

Possible functional significance of the diverse circuitry

The uniqueness of each of the four reconstructed geniculate neurons postsynaptic to the labeled axon need not be surprising, even for the three postsynaptic X-cells. It has been obvious for some time that geniculate projection neurons outnumber the retinal ganglion cells innervating them by a factor of roughly five (Bishop et al., '53; see also Sanderson, '71b). If retinogeniculate circuitry simply amplified the number of geniculate X- and Y-cells relative to their retinal inputs, always by a common rule of retinogeniculate circuitry, then the only purpose served would be redundancy of a straightforward relay of retinal information. Such redundancy might be important if different populations of geniculate projection neurons innervated different cortical areas, but the projection from geniculate X-cells is limited to cortical area 17 (Stone and Dreher, '73; Humphrey et al., '85a,b).

It thus seems plausible that the increase in geniculate neuronal numbers relative to their retinal afferent axons results in an increase in the diversity of cell types available to analyze each region of visual field; there may be an important functional advantage to this instead of merely producing a redundant increase in cell numbers of the same type for such analysis. If so, one might expect most single retinogeniculate axons to combine differently with one another and with other afferent inputs to innervate a heterogeneous population of geniculate neuron. One physiological consequence of such an arrangement could be a range of response properties to a specific visual stimulus (e.g., Mastronarde, '81, '83, '85; Humphrey and Weller, '85). In this manner, geniculate neurons do not act as simple machine-like relays of retinal information and, instead, serve as complex integrators of multiple retinal inputs and numerous nonretinal ones. To illustrate how a single retinal axon can engage in such different circuits innervating geniculocortical projection neurons, we shall again refer to *cells 1-4*.

Cells 1 and 3. The labeled axon provides a significant plurality of retinal synapses to the proximal dendrites of *cells 1* and *3*. Activity in these labeled afferent terminals may well be capable of elevating these cells to threshold for firing, but this input from the labeled axon is generally integrated with that from other retinal terminals. Furthermore, postsynaptic potentials from these labeled and unlabeled retinal terminals are combined with those from the RSD (presumed cortical) and F (presumed inhibitory) terminals to produce the ultimate pattern of firing in *cells 1* and *3*. These cells consequently seem to integrate activity from many afferent sources, including several retinal axons, in the information they convey to cortex.

Cell 2. Although the labeled axon provides the only retinal input seen to *cell 2*, the morphology of this neuron suggests that it is not simply relaying this retinal input to cortex without significant modification. A faithful relay might be indicated if the retinal synapses were close to the soma and not intimately associated with other afferent terminals. Instead, the retinogeniculate circuitry of *cell 2* suggests that the information carried by a single axon is strongly influenced by nonretinal inputs, especially convergent inhibitory inputs to the same appendages from different sources (Hamos et al., '85).

Cell 4. The small number and distal dendritic location of synapses from the labeled terminals on *cell 4* suggest that their functional influence on the cell's firing rate is at best minimal. Nonetheless, the labeled axon repetitively contacts *cell 4*, and it does so selectively while other cells within the terminal arbor are not contacted by the labeled axon. Yet *cell 4* is almost certainly a geniculate Y-cell that is thus innervated, partially at least, by a retinal X-cell axon. Since most reports have emphasized the parallel and separate innervation patterns of geniculate neurons by retinal X- and Y-cell axons (reviewed in Stone et al., '79; Sherman and Spear, '82; Sherman '85a), this is a somewhat surprising observation.

Two different explanations can be considered for this unexpected result. First, it may be an infrequent event in the formation of retinogeniculate circuitry that corresponds to the rare occurrence (<5%) of geniculate neurons with mixed inputs from retinal X- and Y-cell axons (Cleland et al., '71; Hoffmann et al., '72). Second, it may be a frequent concomitant of normal but somewhat sloppy developmental processes. Sur and his colleagues (Sur and Sherman, '82; Sur et al., '82, '84) have suggested that, during normal postnatal development, retinal innervation of the lateral geniculate nucleus by X-cell axons precedes the ingrowth of Y-cell axons (see also Sherman, '85b). As is the case for many early developing pathways (for a review, see Purves and Lichtman, '85), it is possible that the precocious X-cell axons form exuberant arbors and thereby contact an excess number of geniculate cells; these arbors are pruned back competitively as the Y-cell axons arrive to claim their proper postsynaptic sites (Sur and Sherman, '82; Sur et al., '84; Sherman, '85b). Thus, many geniculate Y-cells might first be innervated by a few synapses from retinal X-cell axons prior to the arrival of the Y-cell axons that will subsequently dominate these cells. Any X-cell inputs onto geniculate Y-cells that survive this competitive maturation process, such as that seen from the labeled axon onto *cell 4*, might be the functionally unimportant remnants of an imperfect developmental sequence.

A final point concerns the general lack of synaptic triads seen in the innervation of *cell 4* by the labeled axon. As

noted in Results, this contrasts with other labeled terminals that commonly innervate *cells 1-3* via synaptic triads. Thus synaptic triads are not dictated by the retinal terminals alone, and a retinal X-cell axon is not destined to innervate all geniculate cells predominantly through synaptic triads. This, too, may have a developmental concomitant. Synaptic triads as well as synaptic glomeruli develop relatively late in the geniculate neuropil compared to the appearance of synapses from identifiable retinal terminals (Kalil and Scott, '79; Winfield et al., '80; Winfield and Powell, '80). This may correspond to the rather late development of the presumed GABAergic F terminals that participate in the synaptic triads and glomeruli (Shotwell et al., '84). If, as previously suggested, the terminals contacting *cell 4* are developmental remnants, they were probably formed before synaptic triads could be established.

Selectivity of geniculate circuits related to the labeled axon

As emphasized in Results, the labeled axon is quite selective in its choice of four postsynaptic partners. At least 43 geniculate cells have somata and/or proximal dendritic segments in the ventral region of the labeled axon's terminal arbor, and the number might be substantially higher since we made no attempt to reconstruct all dendrites from nearby somata. The labeled axon is also selective in the distinct mapping of its synapses onto *cells 1-4*. Synapses from labeled terminals are not randomly and equally distributed to these geniculate neurons (Fig. 18). *Cells 1* and *3* receive such synapses throughout most (but not all) of their proximal dendrites (Figs. 6, 12), while *cell 4* receives these synapses on relatively distal dendrites (Fig. 15). There is even a trend for synapses from labeled terminals formed on *cell 3* to occupy a limited portion of the zone of retinal input and more commonly participate in synaptic triads than is the case for unlabeled retinal terminals. Finally, *cell 2* has an especially specific pattern of synaptic inputs from labeled terminals, since these are limited to discrete clusters of dendritic appendages (Fig. 9).

Convergence and divergence of retinogeniculate circuitry

The labeled axon innervates each of the postsynaptic X-cells, or *cells 1-3*, with input that is substantial relative to inputs from other retinal axons. This suggests a limited convergence ratio in retinogeniculate circuitry. These data are entirely consistent with the physiological observations of Cleland et al. ('71), who concluded that most geniculate neurons receive the bulk of their retinal inputs from a small number of axons, often one and occasionally as many as six.

Although we identified only three geniculate X-cells that are innervated by the single, labeled axon, our reconstructions were limited to the ventral portion of the axon's terminal arbor. If we assume that the dorsal, unreconstructed portion of this terminal arbor contains synaptic relationships that are similar to those found in the ventral, reconstructed portion, we can estimate the divergence in retinogeniculate circuitry for the labeled axon. Since the ventral portion of the axon's terminal arbor contains slightly less than one-fifth of all terminal boutons from this axon as estimated from light microscopic observations, we estimate by extrapolation that the axon might innervate

15–20 geniculate X-cells throughout its entire terminal arbor, but that most of these geniculate cells also receive input from other retinal axons. Similar values for other retinogeniculate axons are needed before a better appreciation of convergence and divergence in retinogeniculate circuitry can be realized.

CONCLUSIONS

The results we have described above suggest that retinogeniculate axons, or at least those from X-cells, display both a remarkable degree of selectivity in the number of geniculate neurons contacted as well as considerable diversity in their innervation of these neurons. The selectivity forces important constraints in the elaboration of plausible developmental mechanisms. For instance, the development of this innervation cannot be governed solely by a mechanism that directs an axon to a terminal zone and permits it to innervate all appropriate neurons within that zone. The innervation patterns we have described require a developmental mechanism that can specify innervation at the single cell level. The diversity of these retinogeniculate connections suggests that different functional populations of geniculate projection neurons integrate some of the same retinal inputs into a variety of distinct synaptic circuits involving various other afferent inputs. This permits the lateral geniculate nucleus to transmit to cortex subtly different kinds of analysis for each portion of the visual scene.

ACKNOWLEDGMENTS

We thank Joan Sommermeyer for her exceptional help in preparing the illustrations and Patricia Palam for typing portions of the manuscript. Additionally, we acknowledge Stewart Bloomfield, Josephine Cucchiario, and Daniel Uhlrich for their useful discussions of this work while in progress and for their helpful comments on the manuscript. This investigation was supported by United States Public Health Service grant EY03604.

LITERATURE CITED

- Bishop, P.O., D. Jeremy, and J.G. McLeod (1953) Phenomenon of repetitive firing in lateral geniculate of cat. *J. Neurophysiol.* 16:437–447.
- Bloomfield, S.A., J.E. Hamos, and S.M. Sherman (1985) Passive electrical properties of X- and Y-cells in the cat's lateral geniculate nucleus. *Soc. Neurosci. Abstr.* 11:232.
- Bowling, D.B., and C.R. Michael (1980) Projection patterns of single physiologically characterized optic tract fibres in cat. *Nature* 286:899–902.
- Bowling, D.B., and C.R. Michael (1984) Terminal patterns of single, physiologically characterized optic tract fibers in the cat's lateral geniculate nucleus. *J. Neurosci.* 4:198–216.
- Cleland, B.G., M.W. Dubin, and W.R. Levick (1971) Sustained and transient neurones in the cat's retina and lateral geniculate nucleus. *J. Physiol. (Lond.)* 217:473–496.
- Cucchiario, J.B., D.J. Uhlrich, J.E. Hamos, and S.M. Sherman (1985) Perigeniculate input to the cat's lateral geniculate nucleus: A light and electron microscopic study of single, HRP-filled cells. *Soc. Neurosci. Abstr.* 11:231.
- Dubin, M.W., and B.G. Cleland (1977) Organization of visual inputs to interneurons of lateral geniculate nucleus of the cat. *J. Neurophysiol.* 40:410–427.
- Famiglietti, E.V., Jr., and A. Peters (1972) The synaptic glomerulus and the intrinsic neuron in the dorsal lateral geniculate nucleus of the cat. *J. Comp. Neurol.* 144:285–334.
- Fitzpatrick, D., G.R. Penny, and D.E. Schmechel (1984) Glutamic acid decarboxylase-immunoreactive neurons and terminals in the lateral geniculate nucleus of the cat. *J. Neurosci.* 4:1809–1829.
- Friedlander, M.J., C.S. Lin, L.R. Stanford, and S.M. Sherman (1981) Morphology of functionally identified neurons in lateral geniculate nucleus of the cat. *J. Neurophysiol.* 46:80–129.
- Guillery, R.W. (1966) A study of Golgi preparations from the dorsal lateral geniculate nucleus of the adult cat. *J. Comp. Neurol.* 128:21–50.
- Guillery, R.W. (1967) Patterns of fiber degeneration in the dorsal lateral geniculate nucleus of the cat following lesions in the visual cortex. *J. Comp. Neurol.* 130:197–222.
- Guillery, R.W. (1969a) The organization of synaptic interconnections in the laminae of the dorsal lateral geniculate nucleus of the cat. *Z. Zellforsch.* 96:1–38.
- Guillery, R.W. (1969b) A quantitative study of synaptic interconnections in the dorsal lateral geniculate nucleus of the cat. *Z. Zellforsch.* 96:39–48.
- Hamos, J.E., S.C. Van Horn, D. Raczkowski, D.J. Uhlrich, and S.M. Sherman (1985) Synaptic connectivity of a local circuit neuron in the lateral geniculate nucleus of the cat. *Nature* 317:618–621.
- Hitchcock, P.F., and T.L. Hickey (1983) Morphology of C-laminae neurons in the dorsal lateral geniculate nucleus of the cat: A Golgi impregnation study. *J. Comp. Neurol.* 220:137–146.
- Hochstein, S., and R.M. Shapley (1976) Quantitative analysis of retinal ganglion cell classifications. *J. Physiol. (Lond.)* 262:237–264.
- Hoffmann, K.-P., J. Stone, and S.M. Sherman (1972) Relay of receptive-field properties in dorsal lateral geniculate nucleus of the cat. *J. Neurophysiol.* 35:518–531.
- Humphrey, A.L., M. Sur, D.J. Uhlrich, and S.M. Sherman (1985a) Projection patterns of individual X- and Y-cell axons from the lateral geniculate nucleus to cortical area 17 in the cat. *J. Comp. Neurol.* 233:159–189.
- Humphrey, A.L., M. Sur, D.J. Uhlrich, and S.M. Sherman (1985b) Termination patterns of individual X- and Y-cell axons in the visual cortex of the cat: Projections to area 18, to the 17/18 border region, and to both areas 17 and 18. *J. Comp. Neurol.* 233:190–212.
- Humphrey, A.L., and R.E. Weller (1985) Functional subgroups among X-cells in the lateral geniculate nucleus of the cat. *Soc. Neurosci. Abstr.* 11:318.
- Ide, L.S. (1982) The fine structure of the perigeniculate nucleus in the cat. *J. Comp. Neurol.* 210:317–334.
- Jack, J.J.B., D. Noble, and R.W. Tsien (1975) *Electric Current Flow in Excitable Cells.* Oxford: Clarendon Press.
- Kalil, R.E., and G. Scott (1979) Development of retinogeniculate synapses in the dorsal lateral geniculate nucleus of the cat. *Soc. Neurosci. Abstr.* 5:791.
- LeVay, S., and D. Ferster (1977) Relay cell classes in the lateral geniculate nucleus of the cat and the effects of visual deprivation. *J. Comp. Neurol.* 172:563–584.
- LeVay, S., and D. Ferster (1979) Proportion of interneurons in the cat's lateral geniculate nucleus. *Brain Res.* 164:304–308.
- Mason, C.A., R.W. Guillery, and M.C. Rosner (1984) Patterns of synaptic contact upon individually labeled large cells of the dorsal lateral geniculate nucleus of the cat. *Neuroscience* 11:319–329.
- Mastrorarde, D.N. (1981) Classes of retinal ganglion cells and lateral geniculate cells as functional pathways for visual information. *Invest. Ophthalmol. Vis. Sci. [Suppl.]* 20:97.
- Mastrorarde, D.N. (1983) Subtypes of X relay cells in cat LGN can be distinguished solely by responses to visual stimuli. *Invest. Ophthalmol. Vis. Sci. [Suppl.]* 24:265.
- Mastrorarde, D.N. (1985) Relay cells and interneurons in the cat's lateral geniculate nucleus with excitatory input from more than one retinal X-cell. *Soc. Neurosci. Abstr.* 11:318.
- McGuire, B.A., J.-P. Hornung, C.D. Gilbert, and T.N. Wiesel (1984) Patterns of synaptic input to layer 4 of cat striate cortex. *J. Neurosci.* 4:3021–3033.
- Miles, T.P., and S.C. Rapisardi (1982) Synaptic organization of retinal afferents to class 1 and class 2 thalamo-cortical relay cells in the dorsal lateral geniculate nucleus. *Soc. Neurosci. Abstr.* 8:208.
- Montero, V.M., and W. Singer (1984) Ultrastructure and synaptic relations of glutamic acid decarboxylase (GAD)-immunoreactive neural elements in the dorsal lateral geniculate nucleus of the cat. *Soc. Neurosci. Abstr.* 10:55.
- Parnas, I. (1979) Propagation in nonuniform neurites: Form and function in axons. In F.O. Schmitt and F.G. Worden (eds): *The Neurosciences: Fourth Study Program.* Cambridge, MA: MIT Press, pp. 499–512.
- Peters, A., and S.L. Palay (1966) The morphology of lamina A and A₁ of the dorsal nucleus of the lateral geniculate body of the cat. *J. Anat.* 100:451–486.
- Purves, D., and J.W. Lichtman (1985) *Principles of Neural Development.* Sunderland, MA: Sinauer Associates, Inc.
- Rall, W. (1977) Core conductor theory and cable properties of neurons. In

- E.R. Kandel and S.R. Geiger (eds): Handbook of Physiology, Section 1, The Nervous System, Volume I, Cellular Biology of Neurons, Part 1. Bethesda, MD: American Physiological Society, pp. 39-97.
- Rapisardi, S.C., and T.P. Miles (1984) Synaptology of retinal terminals in the dorsal lateral geniculate nucleus of the cat. *J. Comp. Neurol.* 223:515-534.
- Robson, J.A. (1983) The morphology of corticofugal axons to the dorsal lateral geniculate nucleus in the cat. *J. Comp. Neurol.* 216:89-103.
- Robson, J.A., and C.A. Mason (1979) The synaptic organization of terminals traced from individual labeled retino-geniculate axons in the cat. *Neuroscience* 4:99-111.
- Sanderson, K.J. (1971a) The projection of the visual field to the lateral geniculate and medial interlaminar nuclei in the cat. *J. Comp. Neurol.* 143:101-118.
- Sanderson, K.J. (1971b) Visual field projection columns and magnification factors in the lateral geniculate nucleus of the cat. *Exp. Brain Res.* 13:159-177.
- Sherman, S.M. (1985a) Functional organization of the W-, X- and Y-cell pathways in the cat: A review and hypothesis. In J.M. Sprague and A.N. Epstein (eds): *Progress in Psychobiology and Physiological Psychology*, Volume 11. Orlando, FL: Academic Press, Inc., pp. 233-314.
- Sherman, S.M. (1985b) Development of retinal projections to the cat's lateral geniculate nucleus. *Trends Neurosci.* 8:350-355.
- Sherman, S.M., and P.D. Spear (1982) Organization of visual pathways in normal and visually deprived cats. *Physiol. Rev.* 62:738-855.
- Shotwell, S.L., M.B. Luskin, and C.J. Shatz (1984) Development of GAD immunoreactivity in cat lateral geniculate nucleus. *Soc. Neurosci. Abstr.* 10:142.
- Singer, W. (1977) Control of thalamic transmission by corticofugal and ascending reticular pathways in the visual system. *Physiol. Rev.* 57:386-420.
- Somogyi, P., Z.F. Kisvárdy, K.A.C. Martin, and D. Whitteridge (1983) Synaptic connections of morphologically identified and physiologically characterized large basket cells in the striate cortex of cat. *Neuroscience* 10:261-294.
- Špaček, J. and M. Hartmann (1983) Three-dimensional analysis of dendritic spines. I. Quantitative observations related to dendritic spine and synaptic morphology in cerebral and cerebellar cortices. *Anat. Embryol. (Berl.)* 167:289-310.
- Stanford, L.R., M.J. Friedlander, and S.M. Sherman (1983) Morphological and physiological properties of geniculate W-cells of the cat: A comparison with X- and Y-cells. *J. Neurophysiol.* 50:582-608.
- Sterling, P., and T.L. Davis (1980) Neurons in cat lateral geniculate nucleus that concentrate exogenous [³H]- γ -aminobutyric acid (GABA). *J. Comp. Neurol.* 192:737-749.
- Stone, J., and B. Dreher (1973) Projection of X- and Y-cells of the cat's lateral geniculate nucleus to areas 17 and 18 of visual cortex. *J. Neurophysiol.* 36:551-567.
- Stone, J., B. Dreher, and A. Leventhal (1979) Hierarchical and parallel mechanisms in the organization of visual cortex. *Brain Res. Rev.* 1:345-394.
- Sur, M., A.L. Humphrey, and S.M. Sherman (1982) Monocular deprivation affects X- and Y-cell retinogeniculate terminations in cats. *Nature* 300:183-185.
- Sur, M., and S.M. Sherman (1982) Retinogeniculate terminations in cats: Morphological differences between X and Y cell axons. *Science* 218:389-391.
- Sur, M., R.E. Weller, and S.M. Sherman (1984) Development of X- and Y-cell retinogeniculate terminations in kittens. *Nature* 310:246-249.
- Szentágothai, J., (1973) Neuronal and synaptic architecture of the lateral geniculate nucleus. In R. Jung (ed): *Handbook of Sensory Physiology*, Volume VII/3, Central Processing of Visual Information, Part B, Visual Centers in the Brain. Berlin: Springer-Verlag, pp. 141-176.
- Van Horn, S.C., J.E. Hamos, and S.M. Sherman (1985) Ultrastructure of an X-cell with atypical dendritic morphology. *Soc. Neurosci. Abstr.* 11:233.
- Weller, R.E., and A.L. Humphrey (1985) Structural correlates of functional subgroups among X-cells in the cat LGN. *Soc. Neurosci. Abstr.* 11:318.
- White, E.L. (1979) Thalamocortical synaptic relations: A review with emphasis on the projections of specific thalamic nuclei to the primary sensory areas of the neocortex. *Brain Res. Rev.* 1:275-311.
- Wilson, J.R., M.J. Friedlander, and S.M. Sherman (1984) Fine structural morphology of identified X- and Y-cells in the cat's lateral geniculate nucleus. *Proc. R. Soc. Lond. [Biol.]* 221:411-436.
- Winfield, D.A., R.W. Hiorns, and T.P.S. Powell (1980) A quantitative electron-microscopical study of the postnatal development of the lateral geniculate nucleus in normal kittens and in kittens with eyelid suture. *Proc. R. Soc. Lond. [Biol.]* 210:211-234.
- Winfield, D.A., and T.P.S. Powell (1980) An electron-microscopical study of the postnatal development of the lateral geniculate nucleus in the normal kitten and after eyelid suture. *Proc. R. Soc. Lond. [Biol.]* 210:197-210.